CHALMERS

Dynamic simulation of a centrifugal compressor system

Master of Science Thesis

Johan Liedman
Robert Månsson

Department of Chemical and Biological Engineering
Division of Chemical Engineering
CHALMERS UNIVERSITY OF TECHNOLOGY
Gothenburg, Sweden, 2013

Dynamic simulation of a centrifugal compressor

JOHAN LIEDMAN
ROBERT MÅNSSON

Department of Chemical and Biological Engineering
CHALMERS UNIVERSITY OF TECHNOLOGY
Göteborg, Sweden 2013

Dynamic Simulations of a Centrifugal Compressor
JOHAN LIEDMAN
ROBERT MÅNSSON

© JOHAN LIEDMAN & ROBERT MÅNSSON, 2013.

Department of Chemical and Biological Engineering
Division of Chemical Engineering
Chalmers University of Technology
SE-412 96 Göteborg
Sweden
Telephone + 46 (0)31-772 1000

Deparment of Chemical and Biological Engineering
Göteborg, Sweden 2013

Dynamic simulation of a centrifugal compressor

Johan Liedman & Robert Månsson
Department of chemical and biological engineering
Chalmers University of Technology

Sammanfattning

Ett kompressorsystem från en oljeplattform i Norska havet har simulerats i HYSYS Dynamics™ för att utvärdera en planerad ombyggnad. Modellen har validerats med driftdata från det nuvarande systemet och därefter utvidgats till att simulera kritiska förlopp i det nya systemet. Simuleringarna fokuserar på dynamiska processer såsom uppstart och är avsedd att komplettera befintliga steady-state modeller. Valideringen visade att modellen efterliknar den verkliga dynamiken väl med vissa undantag, t.ex. temperaturprofiler. Vid bedömningen av den föreslagna ombyggnationen av kompressorsystemet, fann man att Anti-Surge-systemet för andra kompressorstegets presterade sämre än väntat. Rapporten illustrerar även andra fördelar med att använda dynamiska simuleringar för processdesign.

Abstract

A compressor system from an oil platform in the Norwegian Sea has been simulated in HYSYS Dynamics™ in order to evaluate a planned reconstruction. The model has been validated with operating data from the current system and then extended to simulate critical events of the new system. The focus of the simulations is on dynamic processes such as start-up and is intended to compliment existing steady-state models. The validation proved that the model mimics the real dynamics well with some exceptions, such as temperature profiles. When evaluating the proposed compressor system redesign, it was found that the anti-surge system of second compressor stage performed below expectations. Other benefits of using dynamic simulations in process design are also illustrated.

Keywords: Compressor, HYSYS, dynamic, simulations, anti-surge, surge, valve

Contents

1 Introduction 1
1.1 Objective 1
1.2 Scope 1
1.3 Thesis overview 2
1.4 Method 2
2 Compressor system theory 3
2.1 Compressors 3
2.1.1 Compressor curves 5
2.1.2 Rotor 7
2.1.3 Driver 7
2.2 Scrubber 8
2.3 Heat exchanger 8
2.4 Piping 9
2.5 Valves 9
2.6 System control 10
2.6.1 Anti-Surge control 12
2.6.2 Scrubber, Heat exchanger and pressure control 13
3 Modeling 15
3.1 Dynamic simulations 15
3.2 HYSYS model 16
3.2.1 Compressor 18
3.2.2 Heat exchanger 18
3.2.3 Boundaries 19
3.2.4 Control 19
3.2.5 Other 20
3.3 Scenarios 20
3.3.1 Scenario A - Shutdown 21
3.3.2 Scenario B – Start-up 21
3.3.3 Scenario C – Step-change 22
4 Validation 23
4.1 Steady State validation – Dataset 1 24
4.2 Steady State validation – Dataset 2 25
4.3 Validation of dynamics, Shutdown – Dataset 3 27
4.4 Validation of dynamics, Start-up – Dataset 4 30

4.5 Validation discussion and conclusions 34
5 Modified design results and analysis 35
5.1 Scenario A - Shutdown 35
5.2 Scenario B - Start-up 42
5.3 Scenario C - Step-change 45
6 Conclusions 52
7 References 53

1 Introduction

Compressor systems are widely used in different applications ranging from refrigeration cycles to industrial chemical manufacturing. One such application is the transport of natural gas in pipelines from offshore oilrigs to the mainland. Even though the pressure of gas and oil obtained directly from reservoirs can be significantly higher than what is needed for transportation, the pressure drop associated with separation and other processing equipment require the gas to be recompressed before exporting. This is done by compressor systems in which several compressor stages can be linked together, also including heat exchangers, separators and anti-surge equipment. Surge is a highly undesirable flow phenomena related to compressor performance in which the compressor can be damaged. Anti-surge systems are therefore used to control the flow and ensure safe operation. (Devold, 2010)

The pressure in a reservoir decreases over time which limits the amount of oil & gas that can be recovered. In order to cope with this problem the compressor system of an existing platform in the Norwegian Sea is planned for modification in 2014 to allow lower pressure production. When designing compressor systems, steady-state models are often used for dimensioning and simulation of predefined steady operation conditions. A compressor system is however often exposed to critical dynamic events such as start-up, shutdown, equipment failure or even mistakes from operators. These types of scenarios were in the past accounted for by experience when designing new systems, but with the development of computational power and higher safety demands dynamic simulations are proving to be an important tool for engineers when designing compressor systems. (Vinod Patel, 2007)

1.1 Objective

The aim of this Masters Thesis is to build a dynamic model of a multistage compression system on an Oil & Gas platform in the Norwegian Sea. This model shall be validated and extended to be used for examining the design of a planned modification of the existing compression system. Further, this thesis should examine possibilities and limitations of dynamic modeling in the applied simulation tool.

1.2 Scope

The scope of this project includes designing a model over the low pressure gas compression part of the mentioned platform in HYSYS Dynamics™ 7.3, and to validate and evaluate this model. This is done with available data from the existing system as well as the basis of the modification. It is beyond the scope to model any other parts of the platform, such as the 3-phase separators and the downstream high pressure compressor system. It is also beyond the scope to fully optimize any part of the modeled systems. The project is also somewhat limited by what the software is capable of modeling.

1.3 Thesis overview

This thesis is structured in such a way that the reader is first introduced to a theory section on general gas compressor systems and then on more specific background information which is needed for assessment of the results. Additional theory, as well as the layout and ideas behind the compressor system model design are introduced in the modeling section. This is followed by the validation chapter, where the results of the model validation are presented and discussed. Finally, results of the modified design evaluation are given in chapter 5 which illustrates the performance of the model with regards to critical parameters.

1.4 Method

Prior to building the model, relevant information of the existing compressor system and modeling theory was acquired. The building of the model was done in stages in order to ensure stability and performance of each part individually before the entire system was connected, starting with the compressor equipment. Data from the documentation of the existing platform was used to make the model as accurate as possible. The model was then validated by simulating specific operating conditions and comparing results with log readings from the platform. The model for the existing system was then remade to simulate and evaluate the design of a proposed modification. This evaluation and discussion encompasses the larger part of the results of this report. Finally, the general possibilities for process tuning and optimization using dynamic models are discussed.

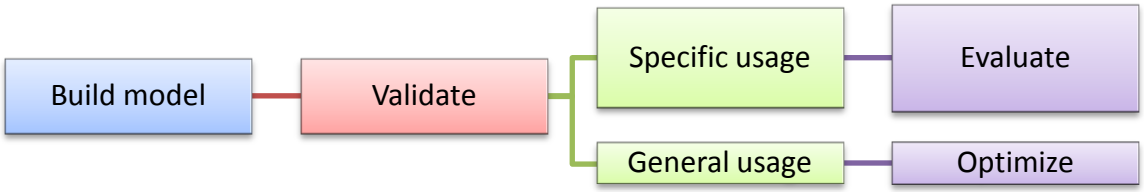

Figure 1 Overall usage of the built model in this thesis, illustrating the different areas of application.

2 Compressor system theory

Compressor systems are widely used in different industrial applications. This thesis concerns gas compression systems found on offshore oil & gas platforms. The main process equipment types used in offshore gas compression system are introduced here and will be further explained in the following subsections.

The unprocessed well flow from the reservoir usually contains a mixture of oil, gas, water and sand which needs to be separated. This is done in 3-phase separators where gravity separates the two liquid phases due to their different densities and the gas is allowed to bubble out. Sediments such as sand and mud are often flushed out with a separate rinsing system. Several separators are often used in stages with decreasing pressure in order to maximize performance while avoiding large pressure gradients.

In order to transport processed natural gas from the offshore platform to the mainland via pipeline, it needs to have a high pressure. Separating equipment and draining of reservoir wells can result in a gas pressure too low for transportation. For this reason, compressors are used to raise the pressure to desired levels. Compressors are relatively sensitive machines and thus extra equipment such as scrubbers, coolers and anti-surge valves are also needed.

Gas scrubbers are used to remove liquid droplets of water and hydrocarbons before reaching the interior of the compressor, where liquid can cause damage to the impellers. Droplet separation can be done either by gravity in centrifugal cyclones, physically by adsorption to demister pads or by absorption in for example Triethylene Glycol (TEG). As gas is compressed its temperature rises and further compression at a higher temperature requires significantly more energy, unless the gas is cooled. This is done in heat exchangers where a mixture of TEG and water often is used as cooling medium. Seawater treated with anti-corrosive chemicals is used to cool this mixture.

For gas compression of large volumetric flow, axial centrifugal compressors with inter-cooling are often used. Several other compressor designs are available and factors such as desired pressure differential, discharge pressure, and flow capacity affect which design that is optimal for a given process. Compressors can be driven by either mechanic or electric energy. (Devold, 2010)

In the remainder of this chapter the different parts of the compressor system is looked into separately in greater detail, starting with the actual compressor itself. It also includes an introduction to the system control that is an important part of any process system.

2.1 Compressors

A compressor is a machine used to compress gas, thereby increasing its pressure. Achieving this pressure increase can be done with two principally different techniques:

- Positive displacement compressors increase pressure by reducing the volume occupied by the gas.
- Dynamic compressors functions by first accelerating the gas to a high velocity and then hindering its movement so that the gas kinetic energy is converted into static pressure.

The two main types of dynamic compressors are centrifugal- and axial compressors. The difference between these two types is the direction of flow through the machine. Centrifugal compressors are among the most widely used compressors in industry and its general design for a single stage can be seen in Figure 2. This report focuses on centrifugal compressors.

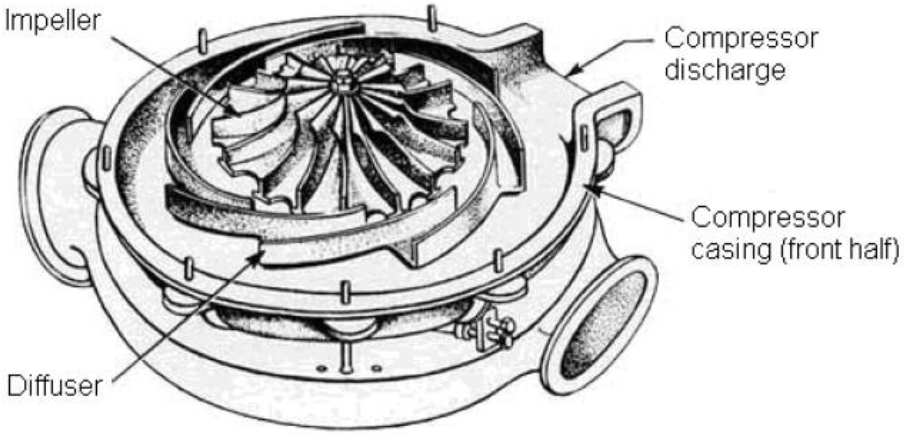

Figure 2 Single-stage centrifugal compressor. (KLM Technology Group, 2011)

After entering a centrifugal compressor, the gas is accelerated outwards by rotating impellers and then de-accelerated in the diffusers before finally leaving through the discharge nozzle. The design of the diffuser generates a circular gas motion preventing surge while converting the gas velocity into increased gas pressure. Centrifugal compressors are often built as series of impeller-diffuser pairs in a single casing where the pressure gradually increases for each pair over the length of the compressor.

The total compressor section from the first impeller to the last diffuser is often called a compressor stage. Thus, a stage is essentially a single multi-impeller compressor. As the gas is compressed, its temperature increases and needs to be cooled in order to avoid gas degradation and damage to the machinery and sealing material. Cooling also reduces the gas volume, which reduces the work (head) needed for a specific compression ratio. For heavy duty systems, two compressor stages can be built in series on a common shaft to allow for cooling of the gas during the compression while using only one motor. This is the case for the compressor system studied in this report and thus it can be seen as a compressor with two compressor stages on a common shaft, separated by an intermediate cooling section and water droplet removal scrubbers. The design of a typical multistage centrifugal compressor can be seen in Figure 3. (Brown, 2005)

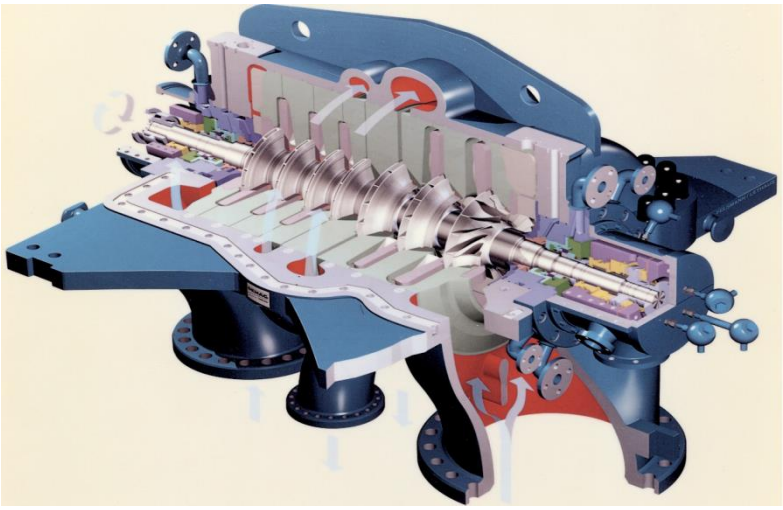

Figure 3 Multi-stage centrifugal compressor. (Bloch, 2006)

2.1.1 Compressor curves

Compressor performance is measured as the amount of change in gas enthalpy achieved from inlet to outlet. As with all thermodynamic processes this change is associated with variations in intrinsic properties such as pressure and temperature. For historical reasons, the change in enthalpy is often noted as "head" in compression and pumping applications and in these cases often in the unit of length. This measurement refers to the height of a liquid column corresponding to a certain pressure differential under constant gravity. Mathematically the enthalpy per unit of mass in SI-units can be converted to the unit of length by dividing with the gravitational acceleration (g);

$$\boldsymbol{Head}\,[\boldsymbol{m}] = \boldsymbol{Head}\,\left[\frac{\boldsymbol{kJ}}{\boldsymbol{kg}}\right] \times \frac{\mathbf{1}}{\boldsymbol{g}\left[\frac{\boldsymbol{m}}{\boldsymbol{s^2}}\right]} \qquad \mathbf{1}$$

The measurement of head can be defined for either isentropic or polytropic conditions. Isentropic processes are both adiabatic and reversible while polytropic processes can be irreversible and thereby have heat losses. The polytropic work is often used to compare compressor performance as this allows one to mathematically separate dynamic losses from the fluid with thermodynamic losses. (ANSYS, 2009) As mentioned earlier, most of the energy used to rotate the shaft and its impellers attributes to the change in pressure. The rest of the supplied energy generates heat by overcoming frictional forces or other losses. For a given shaft speed the amount of work or head generated by the compressor varies depending on the gas flow rate. All compressors are designed to have an optimal efficiency in terms of head for a certain flow rate interval. Data related to performance is often provided by manufacturers in performance curves, such as the one shown in Figure 4.

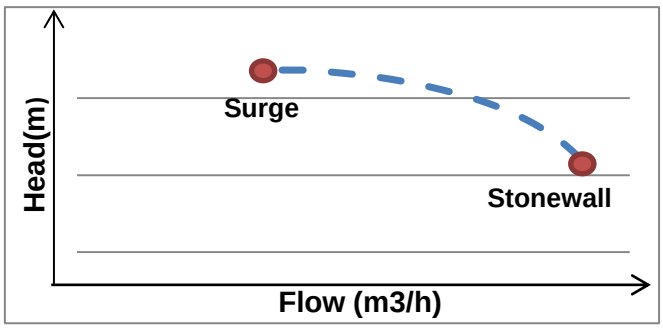

Figure 4 Compressor performance curve showing head vs. volumetric flow for a fixed shaft speed. The surge and stonewall points are highlighted.

As the flow rate decreases for a given shaft speed the compressor eventually reaches the critical surge operating point when flow separates from the impeller or diffuser, resulting in severe fluctuations in performance and potential damage to the machinery. Flow separation changes the gas velocity and direction inside the compressor and causes the flow to become unsteady. The Surge point is the lower limit for stable compressor performance. In order to avoid the problems associated with surge, an anti-surge control system is used to maintain a safe operating volumetric flow through the compressor.

The higher limit in terms of flow rate on compressor performance curves is set by the stonewall point. Stonewall is another term for choking and occurs when no further increase in flow rate is possible as the fluid reaches the speed of sound at a given shaft speed. The result is a significant drop in efficiency due to increased frictional losses at higher flow velocities and possibly mechanical damage. (Peter C. Rasmussen, 2009)

The single curve shown in Figure 4 is defined for a single compressor speed, for variable speed applications compressor curves usually contains additional performance curves for speeds lower than the rated max speed. If performance curves are not available for a specific speed, the Affinity laws (also known as Fan laws) can be used to approximate performance curves for other speeds. These laws express the parameters of flow (Q), head (h) and power (W) as proportional to the speed (N) according to equations 2-4. (Brown, 2005)

$$\boldsymbol{Q \propto N} \quad (2)$$

$$\boldsymbol{h \propto N^2} \quad (3)$$

$$\boldsymbol{W \propto N^3} \quad (4)$$

The average molecular weight of the gas is determined by its composition and will together with temperature and pressure define the gas density. If the gas density is increased for a fixed mass flow rate, the volumetric flow rate will decrease and the compressor head will be increased according to its performance curve. (Golden, 2002) If the pressure ratio over the compressor also is kept constant the compressor will require less torque as less fluid volume is compressed.

Given the wide range in molecular weights operated by gas compressors, this parameter is important to consider when evaluating compressor performance. This means that the compressor curve should be specified to a certain molecular weight. The shaft work needed to deliver a certain pressure ratio is directly proportional to the molecular weight of the gas. (Lapina, 1982)

2.1.2 Rotor

The rotating part of a compressor is called the Rotor and encompasses the shaft, impellers, balancing drum, thrust bearing collar and coupling hub. The shaft is the central rotating beam on which impellers and spacer rings are mounted on. In order to stay stiff and prevent unbalanced rotation, the shaft is often made of high quality steel with high tensile strength. Impellers are designed as a number of vanes radially oriented outwards from the shaft. The vanes are often enclosed on both the front- and backside by cover disks. Impeller vanes for dynamic compressors are normally curved backwards to some extend in order to optimize performance in terms of flow dynamics. (Brown, 2005)

For multi-impeller compressors, the flow volume is being reduced for each impeller as the gas is compressed, resulting in lower efficiency per impeller unless the impeller diameter is decreased in the direction of flow. Doing this would however also reduce the head generated per stage, meaning that additional stages have to be added to maintain the original performance. Adding stages makes the compressor longer and potentially introduces vibrational, dynamic and sizing problems, thus a compromise between efficiency and performance has to be made. (Bloch, 2006)

Power is transmitted from the motor to the shaft from the coupling hub and can be direct or via speed increasing gears as the motor speed is rarely fast enough by itself to drive the shaft directly without gearing. (Brown, 2005)

2.1.3 Driver

The different types of drivers used to power centrifugal compressors can be divided into mechanical and electrical, depending on what energy source they use. Examples of mechanical drivers are those powered directly by a gas turbine or through combustion engines. Electric motors are divided into synchronous or asynchronous types, which differ in how the induced magnetic field that generating torque to the rotor is created. (Brown, 2005)

The torque delivered by the motor to accelerate the compressor (τ_A) is expressed by equation 5 and can be used together with the rotor and gearbox inertia (I) to calculate the acceleration time (T_A) needed to change rotational speed (ΔN) according to equation 6. Here τ_{Tot} is the total torque delivered by the motor and τ_F is the torque absorbed by the compression. It can be noted the torques are not constant during the start-up procedure and that losses, such as friction is not included in equation 5.

$$\boldsymbol{\tau_A = \tau_{Tot} - \tau_F} \quad (5)$$

$$\boldsymbol{T_A = \frac{I * \Delta N}{\tau_A}} \quad (6)$$

The time needed to accelerate the compressor from zero to full speed during startup is important not only for the design of other parts of the process, such as the anti-surge system, but also for dimensioning the motor system as the startup time determines the time an electric motor must withstand max current. (O'Hearn, 2013)

2.2 Scrubber

Apart from the 3-phase separators that are used to separate the unprocessed oil, water and gas mixture, one of the most important separation equipment types on an oil & gas platform is the scrubbers.

A scrubber can refer to different equipment but are often used for a device used to clean a gas stream from pollutants. In offshore gas compression systems, a scrubber is a separator used to separate liquid from the gas stream to avoid droplets reaching the compressor. Other names for the same kind of device include knock-out drum and compressor suction drum.

Different types of internal setups are possible for scrubbers and which one is appropriate depends on the capacity and efficiency required for the separation. The simplest type of scrubber is just an open vessel where the liquid falls down due to gravitation and the gas is taken out at the top. If the gas flow is high and the droplets small they can be entrained with the gas flow and the separation lose efficiency. (Sulzer Chemtech Ltd, 2009) The most common additions into the scrubber internal are demister pads and/or cyclones. Demister pads can often be used with a separating efficiency above 99% and a low pressure drop. A cyclone can be designed for large flows and high pressures/temperatures, but if the velocity is too high (typically above 30 m/s) there can be pick-up of liquid into the gas phase. The pressure drop is also higher when cyclones are used due to the kinetic and friction losses, as well as entry and exit losses. (Sinnott & Toweler, 2009)

A gas-liquid separator can be either horizontal or vertical depending on which phase is dominant. If the gas phase is dominant and there is a low need for liquid hold-up as in the case of a scrubber, a vertical separator is advantageous.

2.3 Heat exchanger

Heat exchangers are used in industry to transfer heat between two different streams. This is usually done by having the two streams flow through the heat exchanger separated by a wall, and the heat transfer occurs by convection between the wall and the flows and conduction through the wall.

The flow through a heat exchanger can be either co-current, meaning the hot and cold streams flow in the same direction, or countercurrent which is when the hot and cold streams flow in opposite directions. Usually a countercurrent flow is preferred as the temperature difference across the heat exchanger, and thereby the driving force, will be larger.

For a single-pass (each fluid flow through the heat exchanger only once) heat exchanger the heat transfer is commonly described by Equation 7.

$$q = UA\Delta T_{lm} \qquad 7$$

Where q is the heat flow rate (W), U is the overall heat-transfer coefficient$\left(\frac{W}{m^2K}\right)$, A is the area ($m^2$) and ΔT_{lm} is the logarithmic-mean temperature difference (K).

It can be noted that the overall heat-transfer coefficient is not necessarily constant over the heat exchanger. For other setups than the single-pass a correction factor, F, can be added to the right-hand side of Equation 7. (Welty, et al., 2008)

The friction inside a heat exchanger can give a considerable pressure drop as the area often is relatively large and the geometry can be complex. For compressor pre-cooling application the heat exchanger commonly used is the tube and shell type, with the gaseous process stream in the tubes and the cooling media in the shell. The pressure drop in the tubes can be calculated in the same manner as in piping.

2.4 Piping

Pipes are used for transportation of fluids and represent an important part of plant design and performance. Piping and Pipelines are generally distinguished by the fact that pipelines are usually much longer than pipes and used in cross-country or offshore delivery. The construction material used for pipes is often chosen from standardized classes of metallic alloys, or in some cases plastics – depending on the area of usage and fluid to be handled.

The most significant impact from pipe design is the reduction in fluid pressure over the pipe. This pressure drop is the result of frictional losses at the interior walls of the pipe and is determined by the choice of constructing material roughness and the pipe length. Bends, fittings and elevations also influence the pressure drop. For dynamic behavior, the pipe volume translates into a hold-up volume that introduces lag and dampens fluctuations in the system.
(Sinnott & Towler, 2009)

2.5 Valves

Valves control or direct the flow of a fluid by partially or fully open or close passageways for the fluid. Valves can be used as safety measures to avoid certain operating conditions, to regulate the flow or pressure of a fluid, or to open up or fully close off a flow. There are many different types of valves that can be used depending on the purpose and the operating conditions of the valve. Manual valves are manually operated and are primarily used to stop or start flow. Valves can also be controlled in a non-manual fashion, either by a separate controller or self-controlled. Self-controlled valves are valves that have a build in control mechanism that allows it to operate without any additional input. Examples of this are relief valves that automatically open when the pressure becomes too high and check valves that only allow flow in one direction. A control valve is regulated by a separate controller and has to include an actuator which can open or close the valve to the position determined by the controller.. The time taken for a valve to go from closed to fully open or the other way around is known as the actuator stroke time. The opening speed of the valve is not necessarily linear during the opening of it.

The size of a valve is often characterized by a flow coefficient (C_v) which is defined by the flow of 60°F water through a valve with 1 psi pressure drop, see equation 8 below:

$$C_v = F\sqrt{\left(\frac{SG}{\Delta P}\right)} \quad (8)$$

Where;
F is the rate of flow in US gallons per minute, SG is the specific gravity (=1 for water at 60º Fahrenheit) and ΔP is the pressure drop in psi.

C_v obviously depends on the opening of the valve and therefore the C_v is given at full opening, as this allows for the largest possible flow through the valve. The relationship between the opening of a valve and the flow (or C_v) through it can be described by the valve characteristics and depends on the geometry of the valve. Common examples of valve characteristics are linear, equal-percentage and quick opening which are shown in Figure 5. Linear characteristics are when C_v increases linearly with the valve opening. Equal percentage is when an equal increment on the opening gives an equal percentage of change in C_v. Quick opening is a characteristic that give large changes in flow for small changes in lift. In reality individual valves are said to have a characteristic even though there are differences to the ideal characteristic. (Fisher Controls International, 2005)

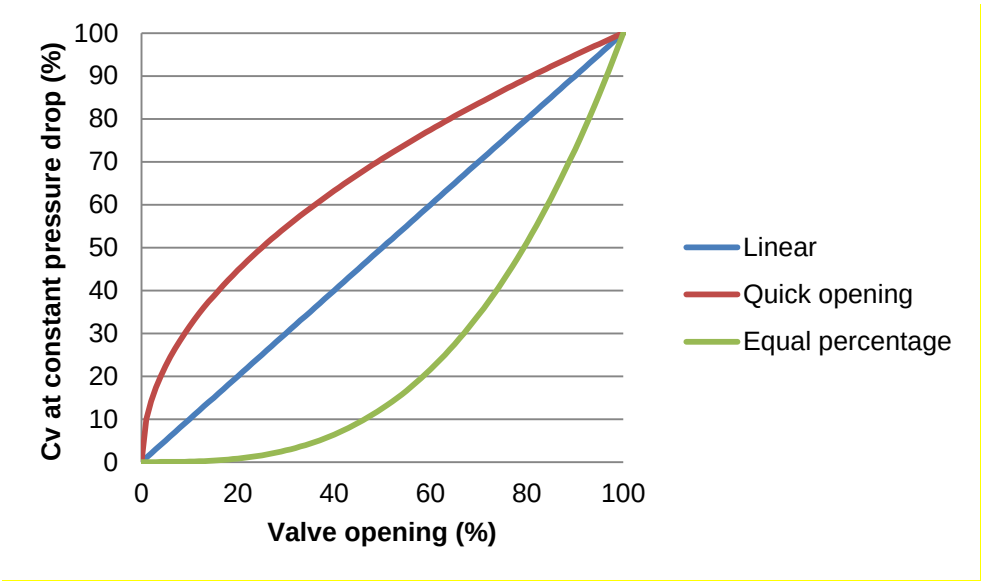

Figure 5 Typical valve characteristics curves for the three most common types. This is the curves used as a standard by HYSYS. (Aspen Technology, Inc., 2011)

2.6 System control

Process control is used to control variables, such as temperature and pressure, in order to ensure stable performance of a dynamic process. This is done by having a controller which can adjust an input to the system. For example, if the pressure is increasing above the set value for a controller the controller can open a valve to release the pressure. The equations that govern the controller can vary between controllers as every system has its own behavior, and therefore require different actions. PID-controllers are very common in the process industry but there are also other more advanced controllers, for example the anti-surge controller for a compressor.

If the set point for a variable, r(t), differs from the real operating value, y(t), it can be said that there is a control error defined as the difference between them. The controller should then be constructed in such a way that the error is eliminated. A PID-controller uses a starting value for the control signal, u0, and the control error to calculate the control signal, u(t). The simplest kind of PID controller is the P-only, which can be described by equation 9:

$$u(t) = u_0 + K_P E(t) \qquad 9$$

Where K_P is a constant, usually called the gain, which is determined for each controller depending on the wanted behavior. A high K_P would give a faster control, with the possible problem of instability that can occur if the whole effect of the control signal is not seen on the operating parameter for the controller instantaneously. A drawback with P-only control is that if the operating conditions are changed the error will not be fully eliminated, as u_0 was designed to give zero error at the standard operating conditions rather than the new ones. (Glad & Ljung, 2009)

If it is necessary to completely eliminate the error another term needs to be added to the control equation. A PI controller is similar to a P-only controller but an integrating term has been added. By integrating the error over time the control signal can be increased until the error is eliminated. The PI controller can be described by equation 10:

$$u(t) = u_0 + K_P E(t) + K_I \int_0^t E(\tau) d\tau \qquad 10$$

Due to the integrating term it will take longer for a PI controller to reach a steady control signal, i.e. it will be slower. (Aspen Technology, Inc., 2011) It will also increase system oscillations as the integrating term uses old information to determine the control signal. As with Kp an increasing value of Ki will lead to a faster reaction of the controller but with an increasing risk of instability, and a longer time to reach a steady value. In Figure 6 below the typical response from a P and a PI controller is shown.

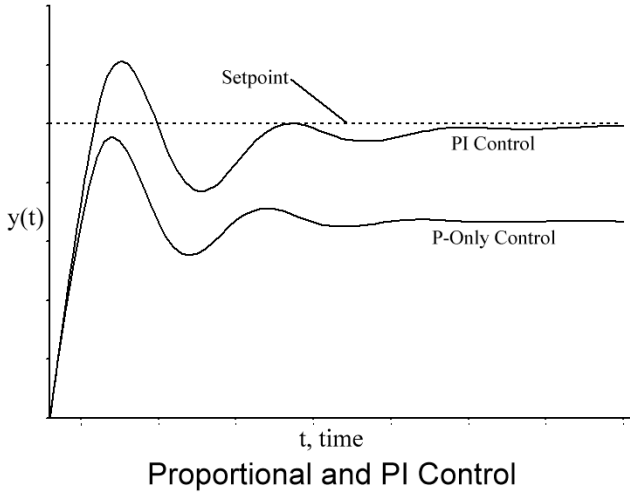

Figure 6 Typical response of a P-Only and a PI controller on a step change (Aspen Technology, Inc., 2011)

Integral windup is a problem associated with the memory of the integrating term when an error is sustained for a considerable length of time. This is particularly a problem when a physical limit is reached, for example when a valve is fully open or closed, and

the error still is non-zero. This windup will then hinder the reaction of the controller when the error is eliminated, with a slow control as the result. Integral windup also results in unnecessary large overshoots when the set point of a controller is changed.

To reduce the oscillation period a derivative term can be added to the controller, giving a full PID controller. By using the derivate of the error the controller can recognize if it is increasing or decreasing and thereby respond more quickly than a controller without derivative action. This can also lead to an increased stability for a controller with derivative action. The output of a PID controller can be described by the equation below.

$$u(t) = u_0 + K_P E(t) + K_I \int_0^t E(\tau)d\tau + K_D \frac{d}{dt} E(t) \qquad 11$$

There also exist other possible forms of a PID-controller equation. It is common in industry to rewrite equation 11 into equation 12 below.

$$u(t) = u_0 + K_P \left[E(t) + \frac{1}{T_I} \int_0^t E(\tau)d\tau + T_D \frac{d}{dt} E(t) \right] \qquad 12$$

Where $K_P/T_I = K_I$ and $K_P T_D = K_D$ accordingly.

It is common in industry to have controllers that does not use the derivative action; one of the reasons for this is that it is not feasible to derivate operating data containing significant levels of interference and noise. (Glad & Ljung, 2009)

In the compressor system there are four different kinds of variables that will be controlled; pressure, temperature, liquid level, and flow (i.e. surge control). For most applications in chemical engineering the PID-controller is sufficient and more complex controllers are unnecessary. The main problem when selecting controller is the tuning of the control parameters. Different methods exist on how to tune a PID controller with rules of thumb in the literature, for example the Zieger-Nichols method. It is common to use such a method, followed by a tune by testing approach. If there exists a good mathematical model of the system to be controlled the parameters can be set more accurately from the start by other methods like the internal model based control (IMC). (Riviera, et al., 1986)

2.6.1 Anti-Surge control

The main goal of the anti-surge control is to prevent the compressor from surging. This is done by having a recycle valve after the compressor that allows flow back to the inlet. It will open if the flow is close to the surge flow and thereby increase the flow through the compressor and prevent surge. As surge can damage the compressor it is important that the anti-surge controller is fast and accurate. Due to the high requirements a more advanced controller than the normal PID is normally used.

The set point of the controller is set to have a defined distance to the surge line of the compressor called the surge margin. The definition of the surge margin varies between different controllers but the idea is to set a value at an appropriate distance from the surge line in order to have a safety margin for the controller. The surge margin is calculated continuously during the operation of the compressor. It is possible to have a backup line closer to the surge line that allows more aggressive action from the controller if passed. Additionally a safety line can be added at surging conditions that if

it is crossed it will increase the surge margin in order to avoid surges in the future. These lines are shown in Figure 7 below. (Brun & Nored, 2008)

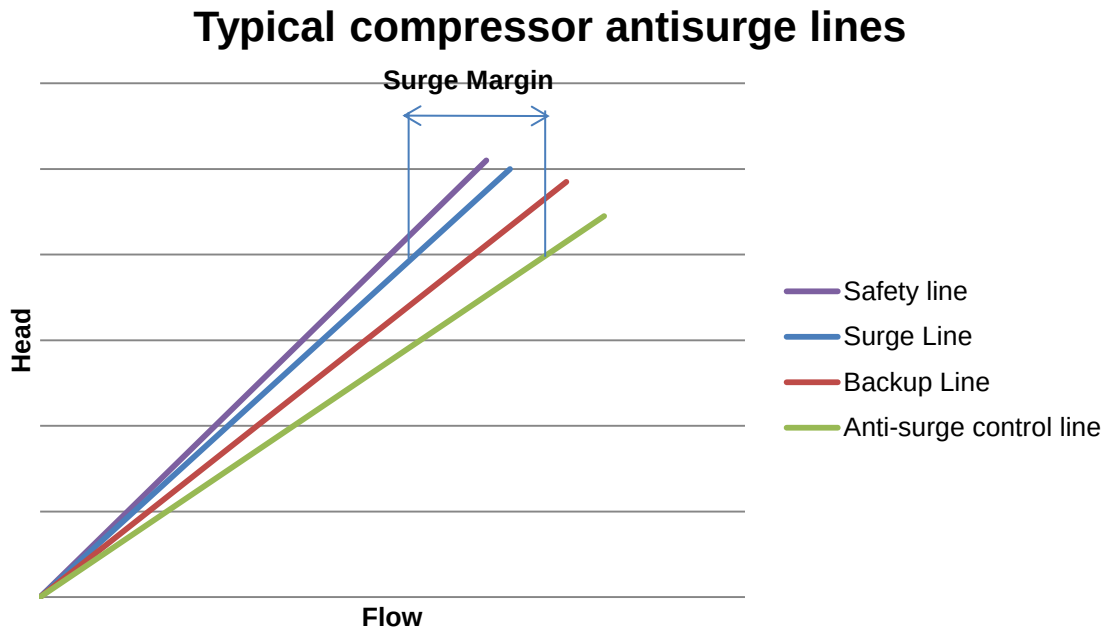

Figure 7 Typical lines for a compressor anti -surge control. The surge line is the actual surge point given by the compressor curves. The other lines are controller lines.

The surge point is dependent on multiple parameters such as the molecular weight and flow into the compressor. In order to describe the surge line it is beneficial to use a coordinate system that is invariant or nearly invariant of the inlet conditions. There are several possible coordinate systems that satisfy the required conditions and one of the most used is reduced polytrophic head versus the reduced suction flow rate squared. Reduced here means that these parameters are recalculated according to equations C1 and C2 in Appendix C. (Bloch, 2006)

The formula used by HYSYS to calculate the surge flow is the following polynomial:

$$h_m = A + B * F_s + C * F_s^2 + D * F_s^3 \qquad 13$$

Where: F_s is the volumetric surge flow, h_m is the head, and A,B,C,D is parameters determined by the user used to relate surge flow with head.

A percentage is then added to the calculated surge flow in order to get the surge margin or the backup line. In HYSYS the controller works as a normal PID controller until the backup line is reached. At this point a more aggressive action is taken by opening the valve with a set percentage per second until the flow is above the backup line again. (Aspen Technology, Inc., 2011)

2.6.2 Scrubber, Heat exchanger and pressure control

The control of liquid level in a vessel is often done with P-only or PI control. The choice between these two is depending on what the aim of the controller is. The P-only controller will have a sustained error in steady-state if the inflow is changed as described earlier. The integrating action can be added to correct this, but the

disadvantage is that the flow of the outlet has larger variations (and overshoot). (Cheung & Luyben, 1979) Normally there is noise inherent with the liquid level control, but if this could be minimized D-action could be included.

The control of temperature in a process stream via a heat exchanger is done by regulating the flow of cooling or heating medium in the equipment. This is often done with a full PID controller, as it is generally desired to have a slow and steady response. If there is noise included the D-action should however not be included.

The inherent process gain related to gas pressure control is generally small and the process response is generally slow, which means that high process gain can be used without large risk of instability. Thus a PI-controller can easily be tuned to control the gas pressure in a system and the derivative action is therefore not necessary. (Aspen Technology, Inc., 2011)

3 Modeling

This chapter will give a general theoretical background to dynamic modeling in HYSYS Dynamics™ and describe the simulated models in detail.

3.1 Dynamic simulations

The difference between dynamic models and steady-state models is that a dynamic model solves the mathematical balances for individual properties such as energy, material and composition as a function of time. This is done by including a time dependent "accumulation"-term in these respective transport equations and differentiating over time. The approximated solution is obtained by numerical integration, as the time-dependent equations are non-linear in nature and thus analytical solutions are hard to find.

HYSYS solves most unit operations by using lumped models, meaning that directional gradients (along the x,y and z axes) are neglected and the solved property is assumed to be constant within each sub-volume. The dynamic behavior of process equipment is based on the fact that they often have a holdup volume, resulting in a time-delay between when changes are introduced at its inlet and when these are seen at its outlet. HYSYS Dynamics™ models the transient system behavior in specific process equipment by using individual holdup models, taking into account their different appearances and functionality. As the delay in response of a property when changes are introduced is a result of accumulation, solving the accumulation term is the key to simulate the response. For this, the holdup model adds a theoretical recycle stream alongside the feed stream which essentially represents the material already existing inside the equipment. The accumulation is then solved according to:

$$\text{Accumulation} = \text{Flow into system} + \text{Recycle stream} - \text{Flow out of system}$$

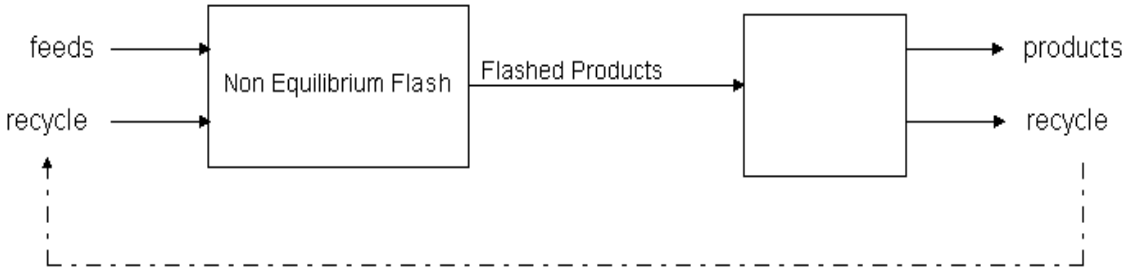

HOLDUP MODEL

In order to reduce calculation times, not every property is solved in each iteration time step. The default settings solves material accumulation every step, holdup energy accumulation every second step and the holdup composition every tenth step.

The assumptions made in the Hysis holdup model are:

- Each phase is assumed to be well mixed.
- Mass and heat transfer occur between feeds to the holdup and material already in the holdup.
- Mass and heat transfer occur between phases in the holdup.

Although each phase is assumed perfectly mixed on their own, this does not include the multiphase mixing between the feed inlet and the existing holdup (recycle stream) if several physical phases are present. For example, the mixing and equilibration of two separate liquid-vapor streams is highly dependent on the internal geometry and residence time of the equipment. The mixing efficiencies governing the multiphase mixing of the holdup volume can be specified in HYSYS and thus the time needed for the holdup volume to reach equilibrium can be altered. If the mixing efficiencies are set low, the system might not have time to reach equilibrium and the product stream can for example contain phases with different temperatures.

Pressure in different unit operations and piping is in HYSYS solved by using resistance equations of the form:

$$Flow = k\sqrt{\Delta P} \qquad 14$$

Here the mass flow rate is described as a function of a specific resistance parameter (k) and pressure drop (ΔP) from friction for a specific unit operation. For a valve, the resistance is modeled by the C_v value.

The Valve unit operation is modeled in HYSYS as two different components: an actuator and a valve. Several options beside C_v are available for the actuator and valve, such as opening time and valve stickiness.

Large rotating parts in for example compressors are exerted to forces due inertia and friction. The effect of accelerating a compressor impeller is important for dynamic simulations and can be modeled by specifying inertia and associated parameters in the HYSYS model for the compressor unit operation. (Aspen Technology, Inc., 2011)

3.2 HYSYS model

The HYSYS model was built in two different versions, the *Existing* and the *Modified*, with the main difference between them being the compressor. In the existing version, which is used later for validation, the data is taken from an existing compressor system on an oil & gas platform in the Norwegian Sea. The second version is based on a proposed future modification of the system with a new compressor for production at lower pressures. In the figure below a simplified schematic of the simulated system is shown.

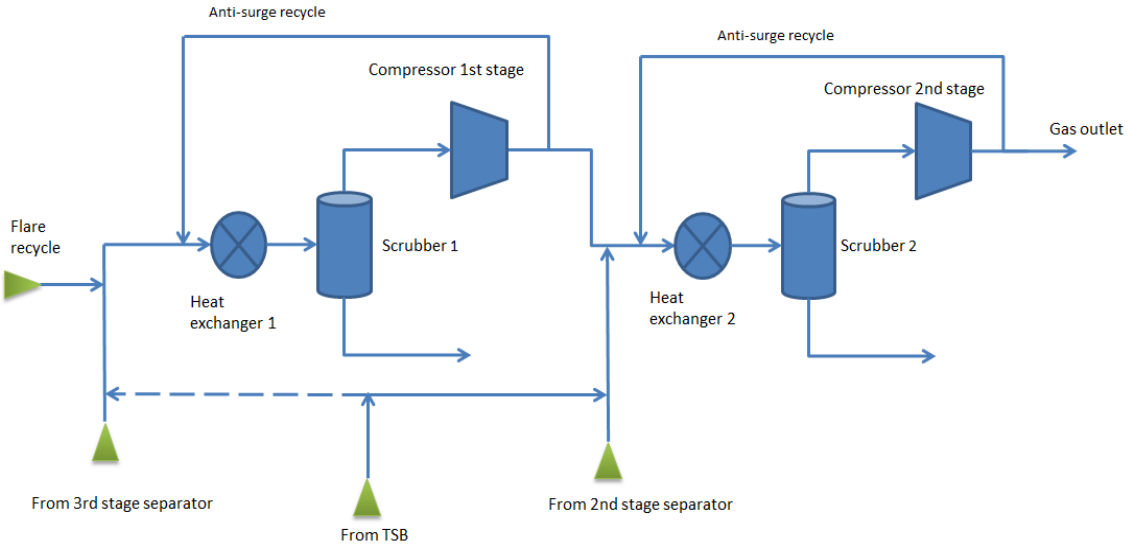

Figure 8 Schematic of the simulated compressor system. A more comprehensive flow sheet of the system is shown in Figure A1 and A2 in appendix A.

The reason for the future modification is to adjust the process for the lower reservoir pressure that is the inevitable result of long time oil and gas extraction. As a result of replacing the compressor, the design inlet temperature and flow is changed between the two systems and therefore the heat exchanger before the first compressor stage needed to be changed. Additionally the possibility of routing the Test Separator B (TSB) to the first stage is added in the modified version (dotted line in Figure 8). TSB is essentially no different from the two other separators used in the model of the gas compression system, but in the entire platform it serves a more flexible purpose than the 2nd and 3rd stage separators.

The modified version operating data comes from a design case for the reconstruction representing normal low pressure gas production. This means producing 20075 sm^3/h (400 tonnes/h) of compressed natural gas of which 17025 sm^3/h (326 tonnes/h) comes from TSB routed to the first compressor stage. The remaining gas inlet comes from the 3rd stage separator (1260 sm^3/h), 2nd stage separator 1070 sm^3/h) and flare recovery (1070 sm^3/h) respectively. Apart from the gas outlet, water is removed from the two scrubbers, which closes the material balance over the system. The pressure from the 3rd stage separator is regulated to 1,4 barg by the flare recovery valve. The 2nd stage separator and TSB are regulated to 6,9 barg in a similar manner. Flare recovery is controlled to 1,2 barg by a valve which is located between the two compressor stages. All the inlets boundary conditions are set as flow specifications, meaning that the pressure can vary if disturbances downstream occur. The gas outlet is however defined by a fixed pressure of 13,7 barg which is the pressure of the real system outside of the model boundary. The molecular weight differs between all inlets as the gas is significantly heavier in the 3rd separator (26,31 g/mole) then in the 2nd stage separator (20,63 g/mole), TSB (19,91 g/mole) and flare recovery stream (18,73 g/mole).

The thermodynamic model used for equilibrium calculations in all simulations was Peng-Robinson, as this model is most widely used for these types of hydrocarbon systems. As Peng-Robinson is best suited for non-polar systems, the model used for the water/TEG mixture in the cooling media side of the heat exchangers was set to NRTL.

Changes were also done to the anti-surge control system between the different versions which will be described in more detail later. Below it will be described how the different parts of the system were modeled and important design choices will be mentioned.

3.2.1 Compressor

Even though the compressor was entirely changed between the existing system and the modified system, the simulations are similar. Both of them have a fixed speed and an electrical motor as the driver. The main data needed to simulate a compressor in HYSYS is the compressor performance curves, the inertias and the driver data.

The compressor curves used in both cases were curves given by the manufacturer of the compressors. As they both are fixed speed compressors the curves was given for only one speed, therefore the affinity laws and HYSYS standard linear extrapolation had to be used for estimation of curves at other speeds in order to simulate the start-up procedure. The existing compressor only had one curve for one molecular weight (for each stage) which was used for all simulations, while the modified compressor had different curves for different molecular weights.

The inertia is important when the speed of the compressor changes as it represents the mass that needs to be accelerated. It is however not important during normal operating of these compressors as the speed is then not varied. The inertia can in HYSYS be given both for the compressor and for the driver motor. The inertia of the modified compressor had not been determined prior to the simulations, and was thus assumed the same as the existing system. The new motor inertia was however given and used in all simulations. The effect of changing the inertia will also be investigated in the results.

The full load speed, gear ratio, power and torque as well as the motor inertia were taken from datasheets for each compressor version. Additionally, a speed versus torque curve for the driver needs to be defined in order to simulate a start-up of the compressor. This data did exist at the time of writing for the existing compressor driver and was implemented. The data for the modified compressor driver was however limited to two points on the curve. Therefore the simulation of the modified compressor used both the old curve and a similar made-up curve with the given two points set.

3.2.2 Heat exchanger

The heat exchanger can be simulated in different ways with different accuracy in HYSYS. In the used model UA is given for a reference flow, and recalculated by taking the ratio between the reference flow and real flow raised to 0,8. This is a basic model and cannot take phase transitions into account, which is present in the simulations. Some simulations were done using a more advanced heat exchanger model but the simulations were slower and the results were unreasonable, and it was therefore rejected.

For the pressure drop over the heat exchanger the *k* value in equation 14 was given for a reference flow. Above the reference flow the *k* value remains unchanged but when the flow is less than the reference flow the *k* value is scaled down by taking the ratio between the flow and the reference flow and multiply it with the given k value.

3.2.3 Boundaries

The system boundaries include the inlets from the three separators and flare gas recovery as well as the gas outlet. Additionally the two liquid outlets from the scrubbers and flare outlets were present. When it comes to mass transfer it is generally recommended by HYSYS to use pressure boundaries, although it is also possible to use flow specification. Additionally temperatures and compositions are needed to be defined for all inlets.

All outlets in the model have their mass transfer boundary condition defined by pressure specifying their pressures. The pressure out of the main gas outlet can be assumed to be independent of the simulated system as the outlet gas get mixed with a much larger flow of gas from the 1st stage separator. In all other outlets the pressures was set to be smaller than the pressure inside the system in order to get a flow through if a valve to it opened.

For the inlets on the other hand the flow was defined instead of the pressure. This is done in order to be able to simulate the volumes before the compressor, and to give more realistic results as a defined pressure can give unreasonable flows. The inlet composition used for the existing version was taken from gas readings when available and from a previous steady state simulation in HYSYS of the system when gas readings were not available. The modified version uses data from the basis of the potential reconstruction.

Even though TSB was included in both models it was not routed into the compressor during any of the simulations with the existing version. The reason for this is that it was routed either to flare or to the second stage outlet for all the available operating data used in the validation. The simulations done with the modified version had TSB routed into the first stage of the compressor for all cases except during start-up.

The walls of piping and unit operation were not simulated meaning the simulation did not include any heat transfer between the system and the surroundings. It did also not include any accumulation of heat in the walls of the system.

3.2.4 Control

The control of the compressor system includes 13 different controllers. All of these were basically simulated the same way, with some special attention taken to the two anti-surge controllers. HYSYS standard controllers were used, meaning that velocity form PID controllers were used. The benefit of using the velocity form instead of a normal PID is that the velocity form does not have any integral windup. The equation for a velocity form PID is shown below, notice that the controller is on a discretized form.

$$u(t) = u(t-1) + K_P\left[\left(E(t) - E(t-1)\right) + \frac{h}{T_I}E(t) + \frac{T_D\left(E(t) - 2E(t-1) + e(t-2)\right)}{h}\right] \quad 15$$

Where h is the size of the time step.

The derivative action was not used in any of the controllers as it easily results in instabilities (especially when velocity form is used), and was not deemed necessary. The control parameters were determined by using the standard recommended values proposed by HYSYS, as the parameters used for the existing system was not available.

For more information on the control system, the different controllers and the control parameters see appendix B.

The surge flow is in HYSYS determined by a polynomial that relates the flow to the head (equation 13). This is adequate for the existing compressor model as the compressor only has one compressor curve. The surge flow of the modified model does however vary with the molecular weight, which makes the polynomial insufficient. The surge flow was therefore instead calculated in a spreadsheet in HYSYS and imported to the surge controller. It was done by putting the surge points in an invariant (not depending on molecular weight) coordinate system using reduced flow and reduced head, and make a regression between the reduced surge flows as a function of the reduced head. The reduced head was then calculated in the spreadsheet which gave the reduced flow which could be recalculated to real flow.

3.2.5 Other

In the scrubber no entrainment of liquid was assumed, meaning full separation is achieved. The dimensions of the scrubbers were taken from datasheets but as HYSYS cannot simulate an ellipsoidal head the height was recalculated to get a cylindrical vessel with the same volume. Also, the internals of the scrubbers were not taken into account.

In order to simulate a valve the flow coefficient (C_v) and the opening characteristics as well as the opening time needs to be given. The exception to this is if the valve does not open or close during operation in which case the C_v is enough. The actuator opening rate was assumed to be linear for all valves. When available data was taken from datasheets, and in other cases typical values were used. This means that anti-surge valve C_v was equal to 200 and 139 for the first and second stage during validation and 245 respectively 110 for the modified version, as suggested by its design. Check valves does generally have a low pressure drop and the C_v was therefore assumed to be high when check valves were simulated.

The volume and pressure drop of the piping was simulated separately which is making it possible to using an equivalent length when calculating the pressure drop. When using equivalent length the pressure loss due to fittings and pipe bends is included in the length. Complete turbulence was assumed for the gas flow, making the *k* value in equation 14 a function of only pipe roughness, length and diameter. The roughness used was a typical value for the roughness of mild steel. Not all the pipes in the system were simulated in order to avoid too much complication and long simulation times. All the pipes in the main system around the compressor stages were however simulated. Exactly which pipes were simulated can be seen in the flow sheet of the system in appendix A.

3.3 Scenarios

Three different scenarios were simulated in the modified model to test the performance of the low pressure production reconstruction before the reconstruction has even begun. The scenarios were chosen according to two main criteria's; to show the dynamic behavior in as many parts of the model as possible and to test the system during as critical performance as possible.

With this in mind, the following scenarios were evaluated:

A. Shutdown
B. Startup
C. Step-change

The following section will give a general description of these scenarios and should provide context to the results presented in chapter 5.

3.3.1 Scenario A - Shutdown

Shutdown of the compressor is the most critical event for the anti-surge system as it requires the largest and fastest response possible to keep the compressor from going into surge. This case is essentially the basis for dimensioning of the anti-surge valves and should give interesting results regarding the performance of the suggested equipment design.

The shutdown is initiated by manually activating one of the alarm trips of the safety control system. This initiates a safety protocol that automatically performs the following actions:

- Turns off the electric motor driving the compressor
- Opens both anti-surge valves fully.
- Closes both scrubber liquid outlets.
- Closes all gas inlet and outlet valves to encapsulate the system, sending the separator flows to the flare system (XV-valves).

The first simulation is meant to show the difference in dynamic response as the system is shutdown while operating at the more liberal base case operating point at 30% surge margin compared to the minimum surge margin (10%) with anti-surge valves fully closed. The minimum surge margin is obtained by reducing the base case TSB inlet flow to 9103 sm^3/h. Shutdown from an operating point very near or at the surge margin and with none to low opening on the surge valves will stress the anti-surge system the most, as this will require the largest and fastest response. It will also be investigated how the tendency to surge is related to the size, and opening time of the surge valve, the compressor inertia, as well as the volume on the discharge side. These evaluations are all done for the more critical case at the minimum surge margin, where the system shutdown from operation at the surge margin with anti-surge valves closed.

3.3.2 Scenario B – Start-up

This scenario is intended to test the performance of the compressor and its motor. The most critical phase of operation for the motor is the start-up of an idle compressor. In fact, the dimensioning of the motor size is often based on the needed torque to accelerate the compressor during start-up. As the new torque-vs-speed curve was unavailable, both an estimated and the existing compressor motor torque-vs-speed curve was used in the simulation of the modified compressor version. The motor and gearbox inertia for the new compressor was however available and used. The full speed of the existing version is 9426 rpm, while the modified version is designed to operate at 10378 rpm.

The validation chapter (4) shows that reasonable results can found when using the affinity laws to extrapolate compressor performance at different speeds. However, as different compressors will have different behavior it is not possible to say for sure that the affinity laws will apply as well on the new compressor as on the existing. Therefore, an estimated version start-up was simulated using both the affinity laws and the linear extrapolation that is default in HYSYS in order to compare the result.

The start-up procedure for the real existing platform was used as basis for preparing the system before starting. This means TSB is routed entirely to flare and flare recovery is not used. Before start-up, the real system is depressurized and then pressurized with natural gas from the 3rd stage separator up to at least 1,4 barg. Immediately after starting the compressor, the 2nd separator inlet valve is opened, pressurizing the second stage of the compressor and increasing its inlet flow. Both anti-surge valves are set to 100% open during the entire sequence, meaning that the anti-surge flow control is deactivated. As the gas from the 2nd stage separator is lighter than the 3rd stage separator, the molecular weight at the second compressor stage inlet will gradually decrease during start-up.

3.3.3 Scenario C – Step-change

The step-change scenario is meant to test the control system response and its ability to adjust to changes in the process. It is also intended to give an understanding of the stability of the entire system. Both scenarios A and B represents cases where the anti-surge valve control is deactivated, as they are both set to fully open during both shutdown and start-up. Thus, this is the only scenario in which the anti-surge control can be evaluated.

The system is initially at steady state at normal low pressure gas production operation (described in section 3.2), with TSB routed to the first stage. The TSB inlet has the largest flow entering the system and this stream was reduced completely in an instant step-change in order to illustrate the behavior and stability of the entire system. After the reduction, the system is allowed to equilibrate and then the TSB flow is returned to full production again in another step-change. Both the 3rd and 2nd stage separators as well as the flare gas recovery were active during the simulation.

Another type of simulation was done to test the control parameters used by the anti-surge valve control. This simulation was intended to compare the Ziegler-Nichols tuning method to “rules-of-thumb” rules and with tuning by “trial-and-error” in the simulation. The rules of thumb were taken from the HYSYS manual, see table B1 in appendix B and used to determine the initial control parameter values for all controllers.

For this step-change the flow from TSB was reduced by more than half (to 4721 sm^3/h) in order to force the anti-surge valves to be open and control the flow prior to the step-change. The step-change was done upwards for the flow control of the anti-surge controller from an operating point of 10% to 30%. This was considered a reasonable large change in order to give distinct results. The C_v and actuator speed values for the anti-surge valves used in the simulation were the preliminary values suggested by the valve manufacturer for the low pressure production modification.

4 Validation

This chapter aims to validate the existing version of the compressor system model used in this report by comparing real data with results from simulations. Different areas of this model will be tested in order to support the discussion of the results in chapter 5 in regards to modeling. The existing version of the compressors system model validated in this section will be the basis for the modified version of the model that is being used for the simulation results in chapter 5.

In order to use a model of a real system to draw accurate conclusions, a critical step is to be able to validate the model. This validation is preferably done by examining the real system and comparing its behavior with the model. The resulting differences found between reality and the model can be caused by many different factors, some which can be accounted for and some that cannot. Obviously one tries to adapt the model to represent the reality as closely as possible, given that the measurements of reality are accurate. Inaccuracies or lack of readings available for validation is a common challenge when building models of processing systems and thus one often has to do the best possible with the measurements available.

As mentioned in chapter 3, the existing version of the model was built to simulate the reality of a platform in the Norwegian Sea. In order to validate this version, four different sets of data were used: two Gas Samplings with steady-state stream compositions and process data from control system log readings done in March 2010 and August 2012. The data from March 2010 was somewhat inconsistent and therefore, two different simulations were done with focus on different parts of the process. For dynamic validation of the system, log data from shutdown and start-up of the compressor system performed in March 2011 respectively January 2012 were used.

Table 1 Available datasets for validation

Dataset	Type	Description	Date
1	Steady-State	Gas Sampling + log readings	August 2012
2a	Steady-State	Gas Sampling + log readings	March 2010
2b	Steady-State	Gas Sampling + log readings	March 2010
3	Dynamic	Control system log readings (Shutdown)	March 2011
4	Dynamic	Control system log readings (Start-up)	January 2012

The log readings include data for pressure and temperature before and after both compressor stages. It also includes flow readings for each stage and the motor power. In addition to this data, the two Steady-State datasets contains measurement of the gas composition at both compressor stage outlets and for dataset 2 also in the separator outlets. The water content of these gas samples were not measured even though the streams do contain water vapor. The unmeasured water content was instead calculated and added in the simulation by assuming saturated gas out of the separators/scrubbers. The reason for this adjustment was that the composition of the gas, and in particular its molecular weight, has a large influence on the compressor system performance.

The measurements of flow rate were done by venturi-meters and the accuracy of this type of calculations are dependent on the actual gas density, as the further away from the calibrated density a stream is, the more error is introduced to the calculation of flow rate. Regarding the head increase delivered by the compressor, the two available performance curves supplied by the compressor manufacturer was defined for a specific

molecular weight of 26,7 and 25,3 g/mole for the first respectively second stage. As these curves were the only ones available, the simulation had to be done using these curves regardless of the molecular weight present in the compressor.

As the gas composition is unknown in the dynamic datasets 3 and 4 the focus will be on evaluating the dynamic behavior rather than comparing differences between measured and simulated values. These measurements have a lower limit of one reading per second, and therefore faster events cannot be studied or validated.

4.1 Steady State validation – Dataset 1

This measurement was done during stable operating conditions with gas entering the system only from the 2nd and 3rd stage separators. This means no flare gas recovery and the flow from Test Separator B is routed directly to flare. Gas compositions were measured at both compressor stage outlets. The results from this measurement and simulations are shown in Table 2. The boundary conditions and controller set points were adjusted in order to obtain conditions close to the measured when possible. The difference between the simulated and measured values is not shown if the variable is directly dependent on boundary conditions.

Table 2 Simulated and measured conditions for dataset 1 (August 2012)

Dataset	Compressor 1st stage			Compressor 2nd stage		
1	Simulated Wet	Measured Wet Calc.	Diff.	Simulated Wet	Measured Wet Calc.	Diff.
Molecular weight (g/mole)	27,92	27,90		27,02	27,05	
Flow (Sm^3/h)	15853	15850		14452	14453	
Inlet pressure (barg)	0,75	0,75		5,58	5,61	**-0,03**
Outlet pressure (barg)	10,59	7,74	**2,75**	13,4	13,41	
Inlet Temp (°C)	40,0	40,2		50,4	50,5	
Outlet temp (°C)	168,1	163,4	**4,7**	108,6	115,6	**-6,9**
Motor power (kW)	2037	2150	**-113**			

It can be seen that there is a difference in both temperature and pressure over the first stage, as well as the temperature over the second stage. Additionally the motor power is larger in the measurement than in the simulations.

4.2 Steady State validation – Dataset 2

The following measurement was performed in the same manner as measurement 1 from August 2012 with no flare gas recovery and Test Separator B routed directly to flare. Gas compositions were measured at both compressor stage outlets and at the outlet from both the second and third separators.

The reported molecular weight readings from the gas sampling in this dataset show a large positive difference between the 3rd separator outlet and the 1st compressor stage outlet. This was considered unreasonable, as the gas exiting the separator should contain a larger fraction water than in the first compressor stage outlet. As water is removed in the scrubber preceding the compressor, the compressor inlet (and outlet) contains less water which increases the molecular weight. Even though some heavier compounds can be separated in the scrubber it was therefore not deemed reasonable that the molecular weight could decrease by the amount seen in the readings. There are several possible sources of errors in the gas composition sampling and measurements, and it is not possible to know which of the two data points is most accurate. Two separate simulations (2a and 2b) were therefore done by matching one of these points per simulation.

Table 3 illustrates the results obtained by simulating the conditions and molecular weight given at the compressor stage inlets (2a) in the same manner as for dataset 1, ignoring the data given at the separator outlets. Numeric differences between simulated results and measurements are given only for parameters that are not directly set by model boundary conditions.

Table 3 Simulated and measured conditions at the compressors for dataset 2a

Dataset	Compressor 1st stage			Compressor 2nd stage		
2a	Simulated Wet	Measured Wet Calc.	Diff.	Simulated Wet	Measured Wet Calc.	Diff.
Molecular weight (g/mol)	27,98	27,94		26,30	26,43	
Flow (Sm^3/h)	15042	15038		12431	12429	
Inlet pressure (barg)	0,62	0,61		5,67	5,68	**-0,01**
Outlet pressure (barg)	8,447	10,0	**-1,55**	13,69	13,7	
Inlet Temp (°C)	41,17	42,4		51,0	50,2	
Outlet temp (°C)	165,4	179,7	**-14,3**	111,0	120,7	**-9,7**
Motor power (kW)	1845	2066	**-221**			

In the 1st stage of the compressor the model underestimates the outlet pressure and temperature, which is the opposite of the results from the validation of dataset 1. The results for the 2nd stage are similar to the results from dataset 1 with a pressure close to equal between the simulation and the measurement but with significantly lower temperature in the simulations.

When the simulation of dataset 2b was done the molecular weight at the separator outlets were set to the same value as the reading. The data for gas flow rates were however only available for the flow inside the compressor, which is governed by the anti-surge recycle. As the size of this recycle stream could not be separated from the total compressor flow for each stage it was not possible to determine the flow of the separator outlet streams. The outlet flow of the separators was instead estimated by using available data of the opening of valves used to control the pressure. This adds additional uncertainty to the simulation of the 2nd stage of the compressor as the flows from the two separators are mixed before going into it.

The temperatures and pressures out of the two separators were also set to the same as in the reading, with the exception of the pressure from the 3rd stage separator which was set by the valve opening of the valve between the two stages. The pressure was lower out of the 3rd stage separator in the simulation which can be either because the flow is too low, giving less loss, or because the pressure drop is underestimated in the model.

Table 4 illustrates the simulation results at the compressor stages obtained when the conditions given at both separator outlets (2b) were defined.

Table 4 Simulated and measured conditions over the compressor for dataset 2b

Dataset	**Compressor 1st stage**			**Compressor 2nd stage**		
2b	**Simulated Wet**	**Measured Wet Calc.**	**Diff.**	**Simulated Wet**	**Measured Wet Calc.**	**Diff.**
Molecular weight (g/mol)	33,24	27,94	**5,30**	30,27	26,43	**3,96**
Flow (Sm^3/h)	15060	15038		12380	12429	
Inlet pressure (barg)	0,65	0,61	**0,04**	4,98	5,68	**-0,7**
Outlet pressure (barg)	14,35	10,0	**4,35**	13,72	13,7	
Inlet Temp (°C)	41,7	42,4		50,9	50,2	
Outlet temp (°C)	173	179,7	**-6,7**	112,4	120,7	**-8,3**
Motor power (kW)	2180,4	2066	**114,5**			

As can be seen, the major differences to the measured data at the compressor are the molecular weights for both compressor stages and the outlet pressure of stage 1. The temperatures are too low in this simulation, which is in line with the results from the previous simulation. It can also be seen that an error of the pressure into the 2nd stage

compressor has been introduced. Comparing the results from Table 3 with Table 4 shows that the increased molecular weight and larger pressure differential for the first stage results in a larger motor power for the dataset 2b simulation.

4.3 Validation of dynamics, Shutdown – Dataset 3

This section compares data between an actual and a simulated shutdown. All readings preceding the shutdown is within the allowed operating margins. The shutdown is assumed to be representative for a general shutdown of the compressor system at the platform.

The aim of the shutdown simulations was not to imitate the reality as closely as possible as there was not enough data to accurately do so. The simulations were instead done with probable estimation of the operating conditions. This led to that the comparison between the real and simulated data had to be done in mainly terms of the general behavior. The molecular weight for the simulations was 28,80 for the 1st stage and 25,56 for the 2nd, and the surge margin was set to 20% by the anti-surge controller.

For the shutdown simulations it was observed that the speed (rpm) of the compressor increased shortly after a surge event. This is an error in the calculations related to the extrapolation of compressor curves outside of the known flow range. As both compressors are on the same shaft the increase will affect both stages even if only one of them goes into surge.

In Figure 9 below the standard volumetric flow is shown for both the real system readings and the HYSYS simulations over the two stages. In the simulation both stages reached surge conditions closely after the shutdown.

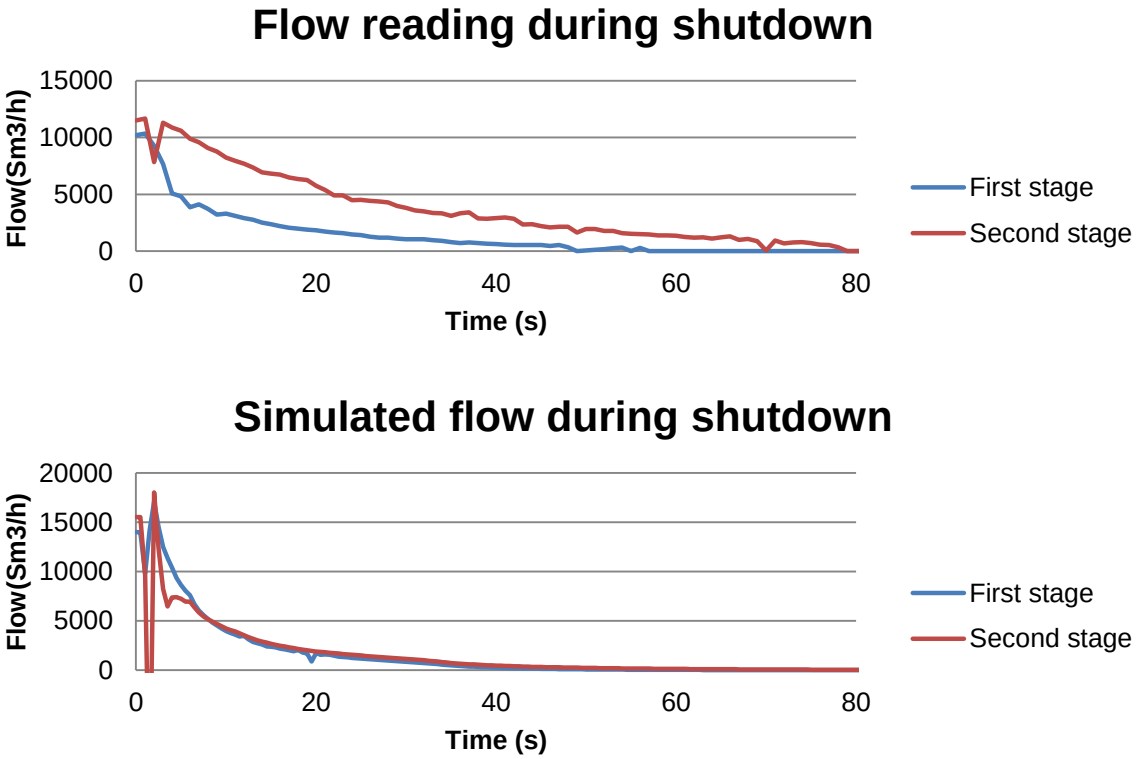

Figure 9 Standard volumetric flow versus time for shutdown from measurement (top) and a simulation (bottom) for the two compressor stages.

The readings show no indications of surge in the 1st stage but a possibility of surge in the 2nd stage. The simulation does however surge in both stages and the event is more aggressive than in the readings. The controller surge margin set point was relatively high (20%) during the simulation which mean that a too low distance to surge should not be the main reason for the higher tendency for the simulation to surge. Other possible reasons include differences in the surge valve opening times and sizes. The volume at the compressor stage discharges is also of importance. All these parameters will be further investigated during the shutdown scenario simulations. After the surge event there is an overshoot in flow through both stages. This is not expected, but is assumed to be related to the HYSYS extrapolation error during surge leading to an increase in compressor speed as mentioned earlier. Additionally it can be seen from the figure that the reduction in flow is faster in the simulations than in the measurement.

The data of the stroke times for the anti-surge valves for the existing system were particularly uncertain. Thus, a second simulation was done in order to investigate the effect of having a faster opening speed. An instantaneous actuator was used for this simulation, as this is the case that has the largest possibility to avoid surge. The results are shown in Figure 10 below.

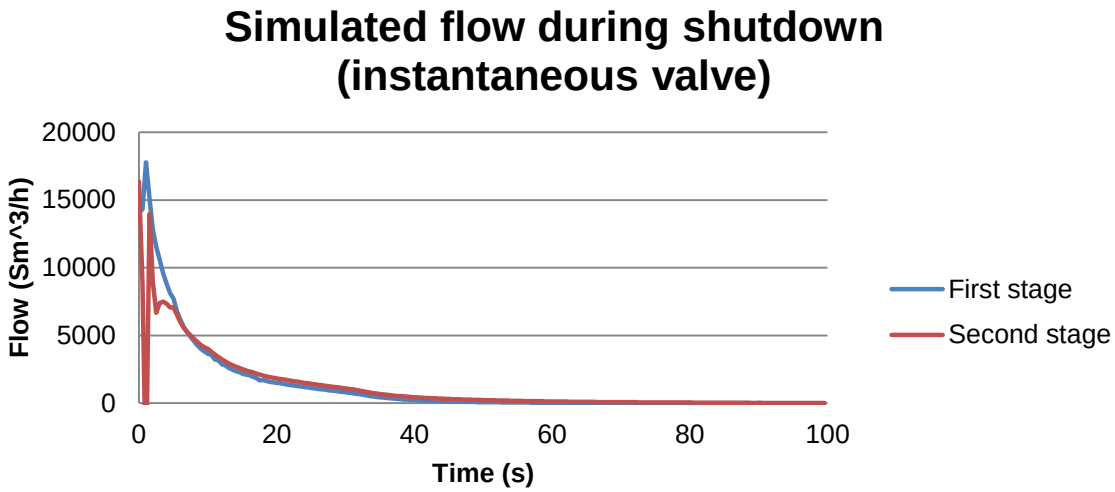

Figure 10 Standard volumetric flow versus time for shutdown from simulation with instantaneous surge valve for the two compressor stages.

The behavior can be seen to be very similar to the previous simulation, with the main difference that the first stage never reaches surge. The overshoot seen for the 1st stage is partly explained by an increased flow through the surge valve when it opens instantaneously after the shutdown is initiated. It is also plausible that the overshoot is related to the calculations for the surge event in the 2nd stage, in the same manner as before. The difference in the surge over the 1st stage does not seem to affect the time for reduction in flow considerably.

In Figure 11 the pressure over the compressor stages is shown as a function of time during the shutdown.

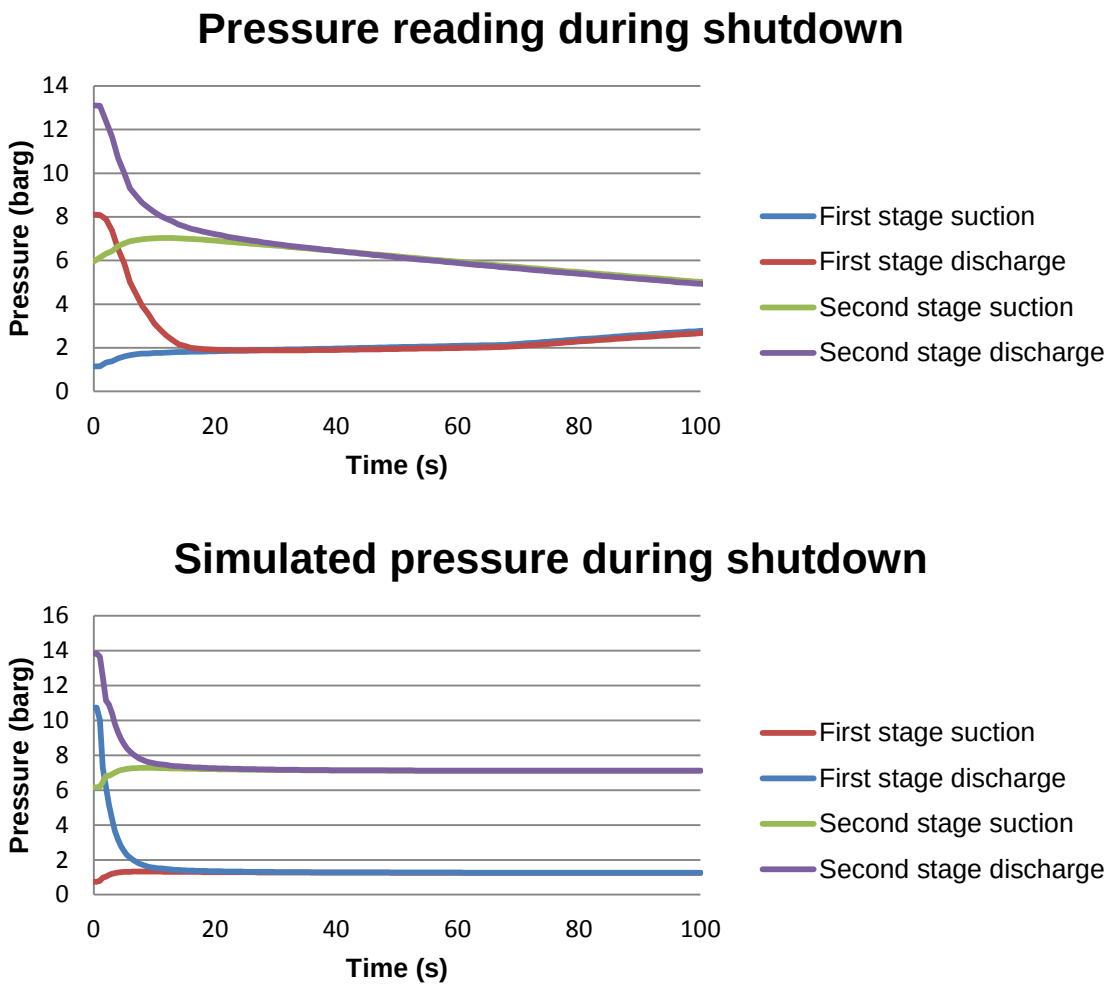

Figure 11 Pressure versus time for a shutdown from measurement (top) and simulation (bottom) for both sides of each compressor stage.

There are two effects shown in these graphs; firstly when the pressure equalizes over each stage, and secondly when the pressure equalizes between both stages. The second effect is responsible for the pressure convergence seen in the real system. In the simulations there is no leakage between the stages, which is the reason that the second effect cannot be seen in the simulation. The first effect is similar between the readings and simulations, but possibly a bit faster in the simulations.

The temperature at the suction and discharge of the compressor is shown in Figure 12 below. Observe that the time scale is different for the readings and the simulation.

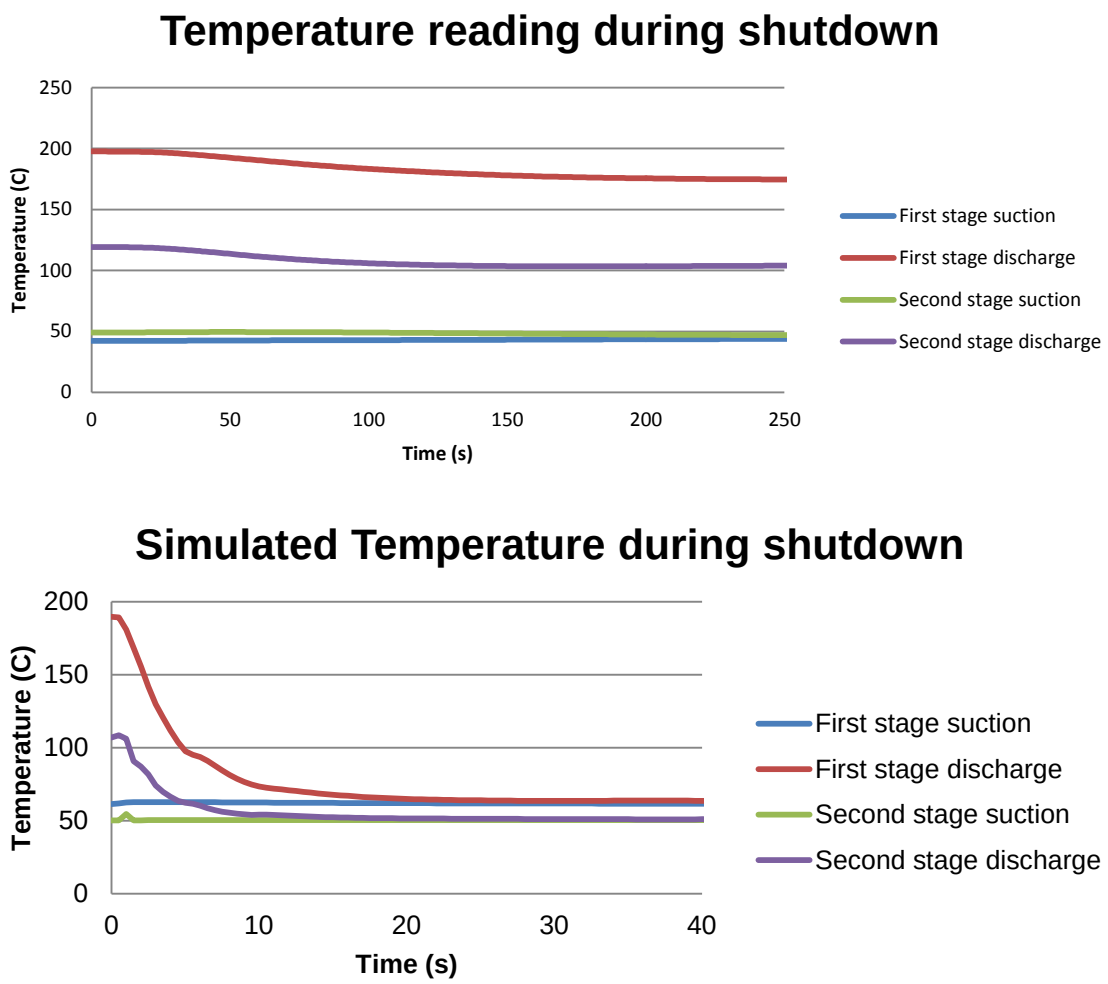

Figure 12 Temperature versus time for a shutdown from a measurement (top) and a simulation (bottom) for both sides of each compressor stage.

It can be seen that the temperature profile during the shutdown is not at all similar between the readings and the simulation. This is because of accumulation of heat in the walls of the system is not simulated. The accumulation of heat is responsible for two different effects on the results in these graphs. The first is that the flow will keep a higher temperature as heat is exchanged from the wall into the gas, giving a slower temperature decrease in reality than in the simulations. The other effect is that the temperature of the measurement device will be kept higher than the gas as it is embedded into the wall, which would lead to that the temperature decrease in reality is faster than in the measurements. This is especially true as the flow and thereby the heat exchange between the gas and the thermometer is decreased.

4.4 Validation of dynamics, Start-up – Dataset 4

This measurement represents readings from a start-up of the compressor system from operating conditions resembling those of the operating guidelines for compressor start-up. The separator outlet flows were not supplied in dataset 4 and therefor these were assumed to be 1094 sm^3/h and 910 sm^3/h for the 3^{rd} and 2^{nd} stage separators respectively. These inlet flows should have a small impact on the results from the simulations as the available volume in the system is large and as the anti-surge valves

are fully open. Large parts of the flow going through the compressors are recycled through the anti-surge valves. The molecular weight at the beginning of the simulation was set to 27,3 g/mol in the whole system, but decreased during the start-up as molecular weight of the inlet from the 2nd stage separator was lower and because some heavy components was separated in the scrubber. The molecular weight after 60 seconds over the compressor stages were 25,8 and 26,4 g/mole respectively. The anti-surge valve was fully opened for both stages during the whole event.

One of the most important validation data is the time it takes for the compressor to reach full speed. Simulation gives a start-up time of 6,5 seconds, while the real system takes somewhere between 5 and 7 seconds. It can be seen that the simulated start-up time is in the interval of the real start-up time.

Figure 13 illustrates the volumetric flow through both compressor stages. As the flow rate into the system was not known in dataset 4, a comparison between the numeric values flow between two cases is a bit uncertain. The trend shows the dynamic behavior of both cases and can be compared.

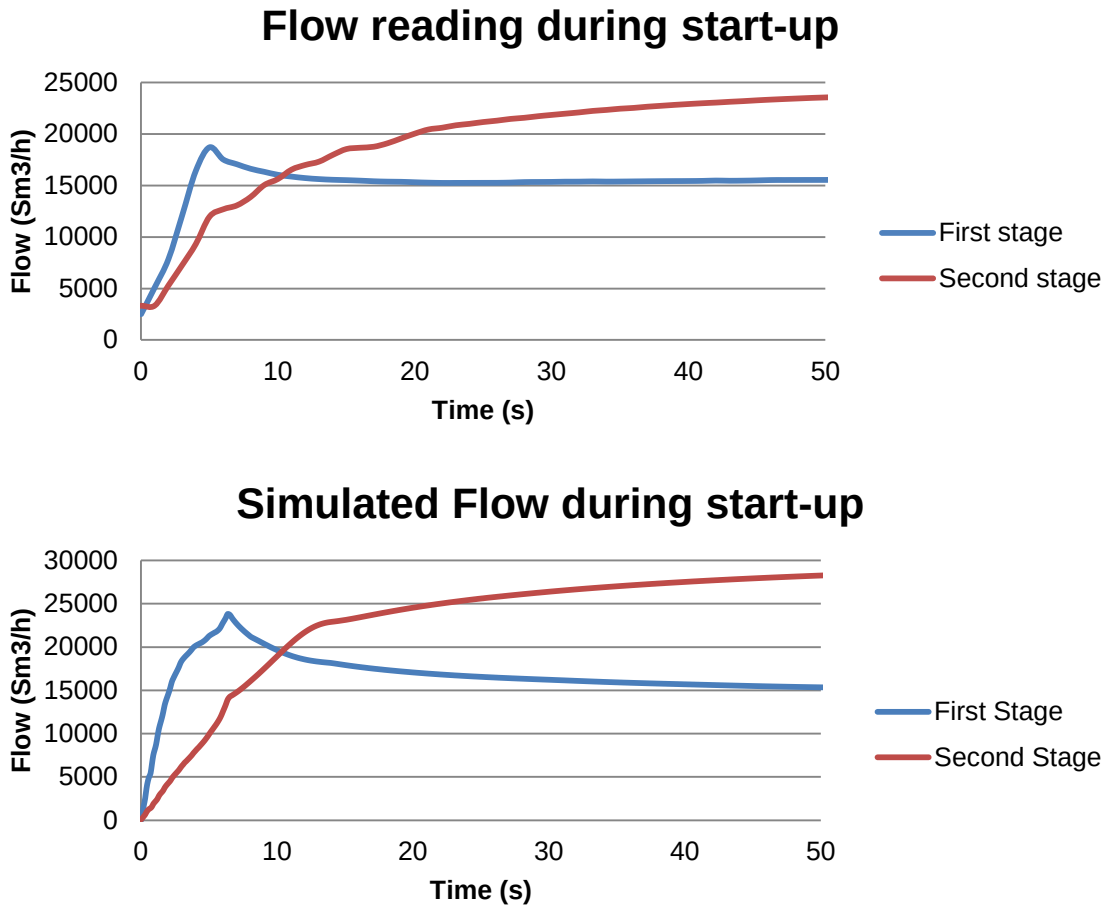

Figure 13 Flow measured and simulated for both compressor stages during start-up of the system.

The trend is very similar between the readings and the simulation over both stages, with the main difference being the behavior close to the flow peak in the first stage. The flow is generally larger in the simulations which, beside a possibly larger inlet flow to the system, could be related to the way stonewall is simulated. The simulation reaches stonewall during start-up and since the model does not limit the flow at the stonewall

flow it can be overestimated in the simulation. The modeling of stonewall could possibly also affect the shape of the flow peak in the first stage.

Figure 14 shows the pressure in the system for both cases with the system pressure prior to start-up at 1,7 barg according to the dataset. As it is not known what molecular weight that was present in the readings the numerical values should not be compared.

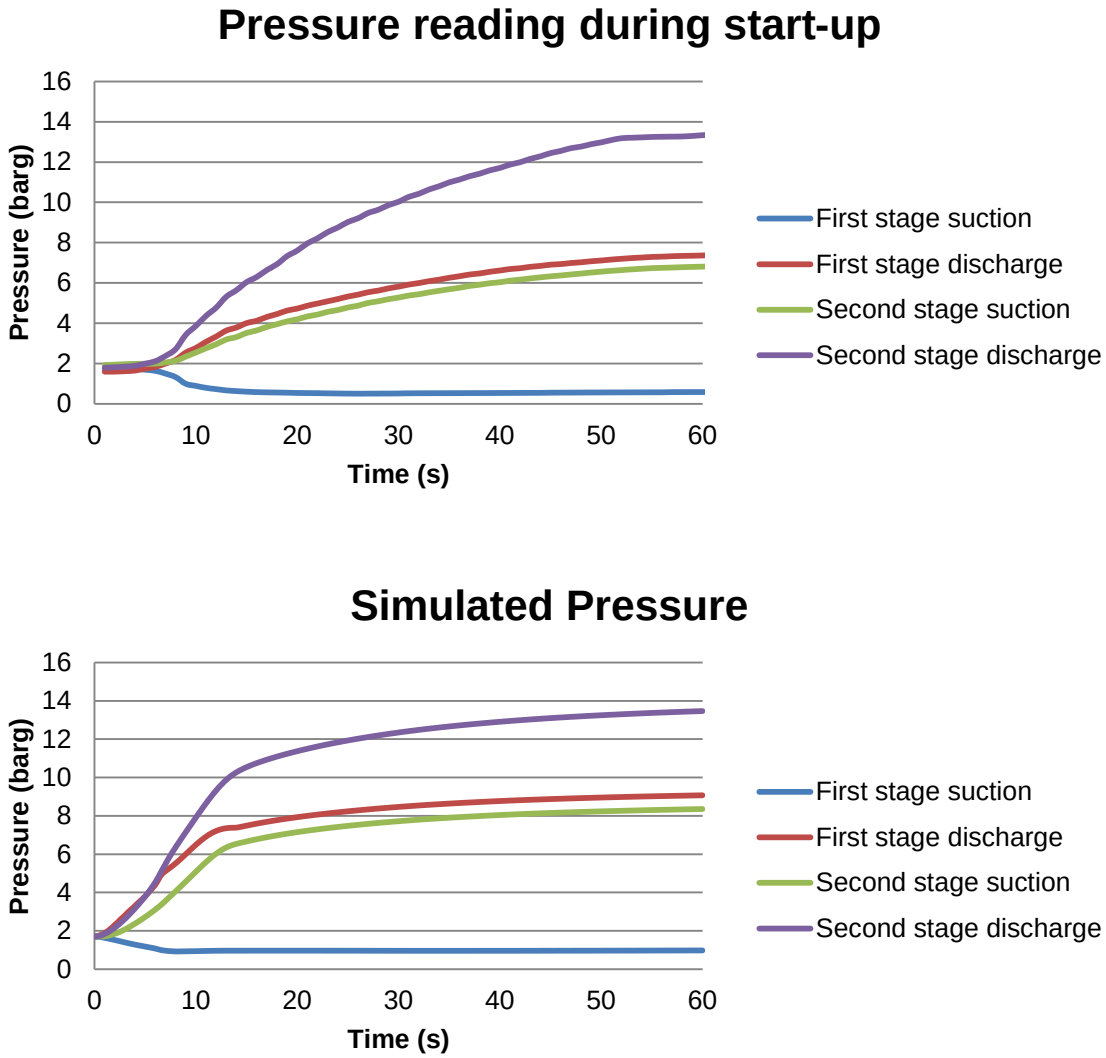

Figure 14 Pressure for the measured case and simulation during start-up of the system for both compressor stages.

The transient result for start-up differs to the readings in a similar manner as in the shutdown scenario dynamic validation in section 4.3 as the overall behavior is quicker in the simulation. The pressure difference between the first stage discharge and the second stage suction is significantly larger in the beginning of the simulation. One explanation for this is that the affinity laws could overestimate the fluid torque during the start-up and hence increase the pressure faster than in reality. Other possible reasons for these include overestimated flow resistance between the stages and that inter stage leakage was not simulated. The internal volume of the system can also affect the rate of pressurization thus the simulated volume might not correspond to the real system accurately enough.

Figure 15 shows the temperature gradients in the system during the start-up procedure. These values can also be compared as temperature readings were available in the dataset.

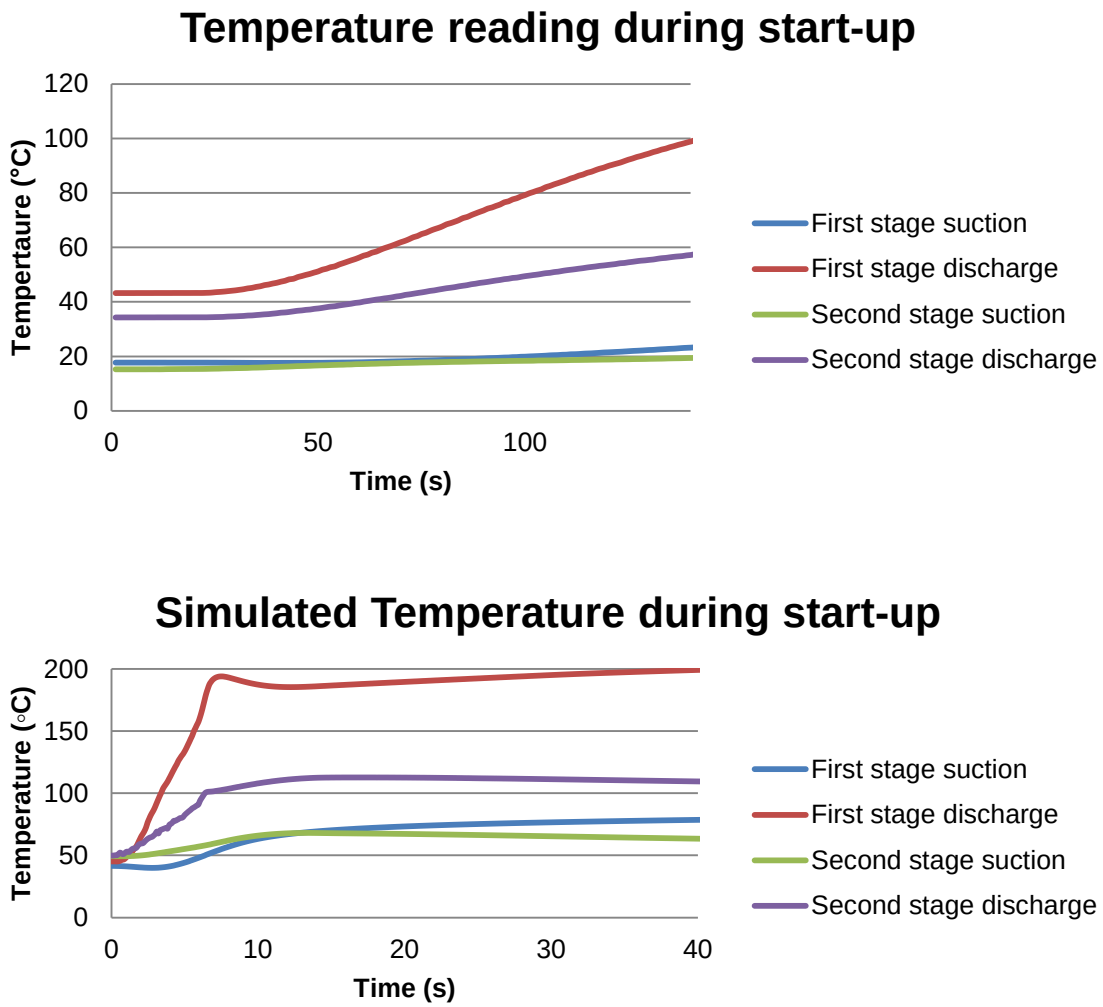

Figure 15 Temperature measurement and simulation during system start-up at both sides of both compressor stages. Notice the difference in timescale for the simulated case.

This data shows large difference in response between the readings and simulations. This is similar to the result from the shutdown event and expected as the heat transfer from the wall is not simulated as discussed earlier in section 4.3. The initial temperature is higher in the simulation as the way the system is prepared and pressurized prior to the start-up does not allow for separate temperatures for the compressor stages.

4.5 Validation discussion and conclusions

From the steady-state validation it can be seen that the molecular weights are of great importance for the simulated performance of the compressor. As the measurement of this property was uncertain, this data could not be compared as well as desired for the steady state validation. The model did however overestimate the discharge pressure with the largest suggested molecular weight (2b) and underestimate it with the lowest suggested weight (2a), which is a reasonable behavior.

It can also be seen that the temperature out of the compressor stages are underestimated in almost all steady state simulations. This indicates that the curves used for the polytrophic efficiency is overly optimistic. Assuming that the compressor curves were correct for the compressor when it was new the probable reason for this is fouling and wear of the compressor. Given the inaccuracies mentioned in the steady-state measurements it is hard to draw conclusions from the overall steady-state validation. It is however not unlikely that the model is reasonable accurate for a given molecular weight.

During both start-up and shutdown, changes in flow, pressure and temperature consistently occurred faster in the simulation compared to the log readings. This is true for both pressure and temperature and indicates an underestimation of the different resistances in the system and/or compressor curve extrapolation errors. These resistances can include volumes, pressure-drops and friction losses in both equipment and piping. For the temperature roll-out this difference is significantly larger, as heat transfer and accumulation in walls has not been simulated. Also, the initial temperature of the start-up was lower in the readings than simulated.

The start-up time was similar between the measurement and the simulation which indicates any inaccuracies in affinity law extrapolations were small enough for this parameter to show similar results, as the fluid torque (and thereby start-up time) is affected by the extrapolation of the compressor curve at different speeds.

In general the model behaves similarly to the measured data which indicates that the model can be used to study the behavior of the system. Attention should however be kept on when and what the model is less capable of simulating. This mainly includes fast temperature changes, compressor performance during and after surge, and the time for events to happen. As resistances can be underestimated there is a larger risk of effects appearing to be amplified in the simulation, as the damping effect of resistances is not as strong. The importance of the accuracy of the different compressor curves and other data changed between the versions also should be noted.

5 Modified design results and analysis

The previous section on model validation highlights the strengths and weaknesses for the model of the existing compressor. In this chapter, a modified version of the existing compressor model is used to simulate 3 different scenarios, in order to evaluate and predict performance of the following critical system components for the planned reconstruction. These results are presented and discussed in the following subsections. The modifications of the existing system are described in the modeling section (3).

5.1 Scenario A - Shutdown

This scenario simulates a shutdown of the entire compressor system from normal gas production and is described in greater detail in chapter 3.3.1. The focuses in this evaluation is on whether the anti-surge system can handle the event without going into surge. For this, the following parameters were varied and evaluated as these affect the tendency for the system to surge:

- Surge margin
- Anti-Surge valve C_v
- Compressor inertia
- Discharge volume
- Actuator opening speed

In Figure 16 the trail of the operating point during shutdown is shown as solid lines. The compressor performance curves that matches the molecular weight during the simulation is included in the figure as dashed lines. The lower two compressor curves are downscaled with the affinity laws from the given curve. The surge line will follow the left-most points of the compressor curves and the operating point will travel from the full speed compressor performance curve downwards towards the origin during a shutdown.

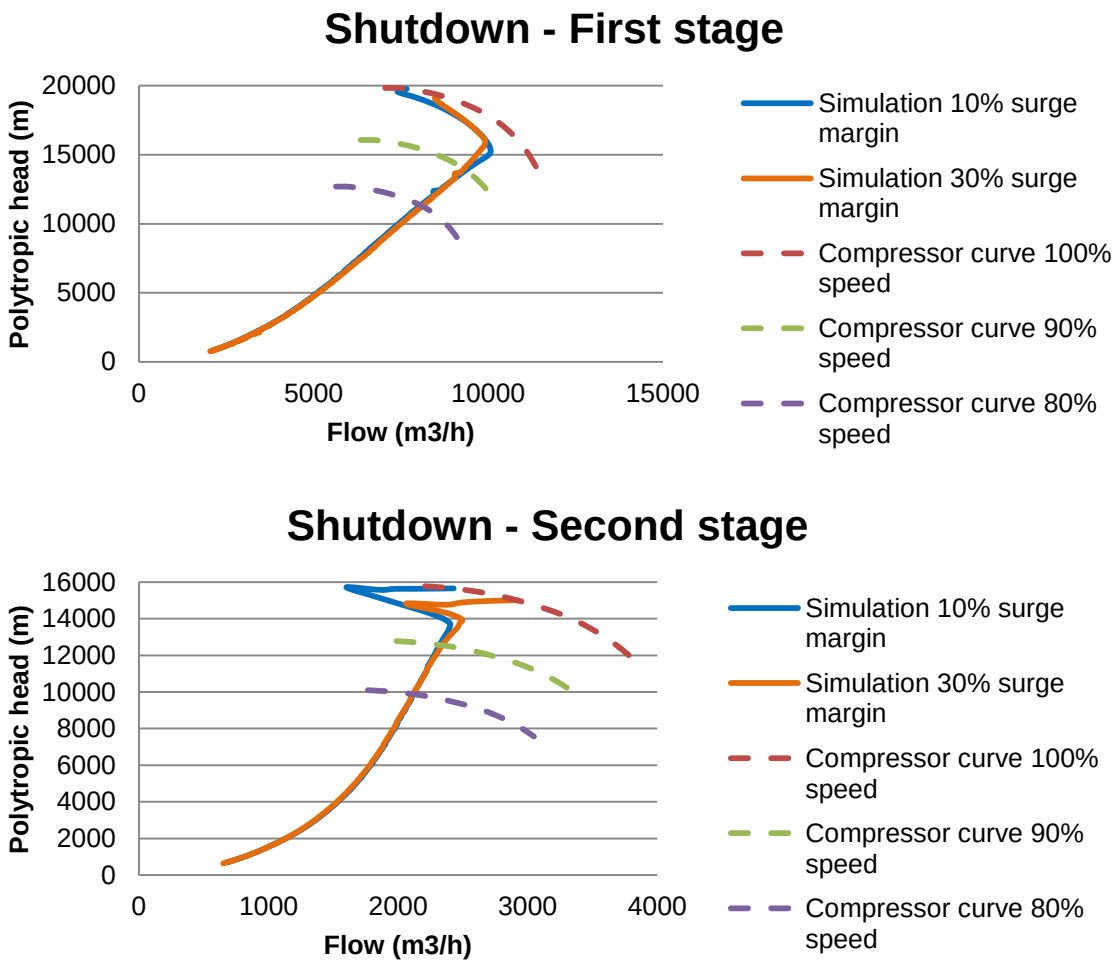

Figure 16 Compressor performance during shutdown of the system from normal production at 10% respectively 30% surge margin.

The trail over the first stage of the compressor behaves as expected; the flow decreases directly after the compressor is turned off but increases again as the anti-surge valve opens, before it eventually dies out. A similar event is seen over the second stage when starting at the 30% surge margin, as the increase in flow does just barely manage to hinder the operating point to go over into the area representing surge. When the operating point is set closer to surge line prior to the shutdown the event will be even more critical, as the system has less time to react to the sudden change in operating conditions. With the lower margin to surge the first compressor stage is closer to surge but does manage to avoid it. The second stage however, does not manage to avoid surge for the 10% surge margin simulation.

One way to improve the anti-surge system is to increase the size of the anti-surge valves. This effect was evaluated and is shown in Figure 17 for both compressor stages. The C_v value for these valves was varied ±10% from the value suggested by the preliminary design of the new compressor system.

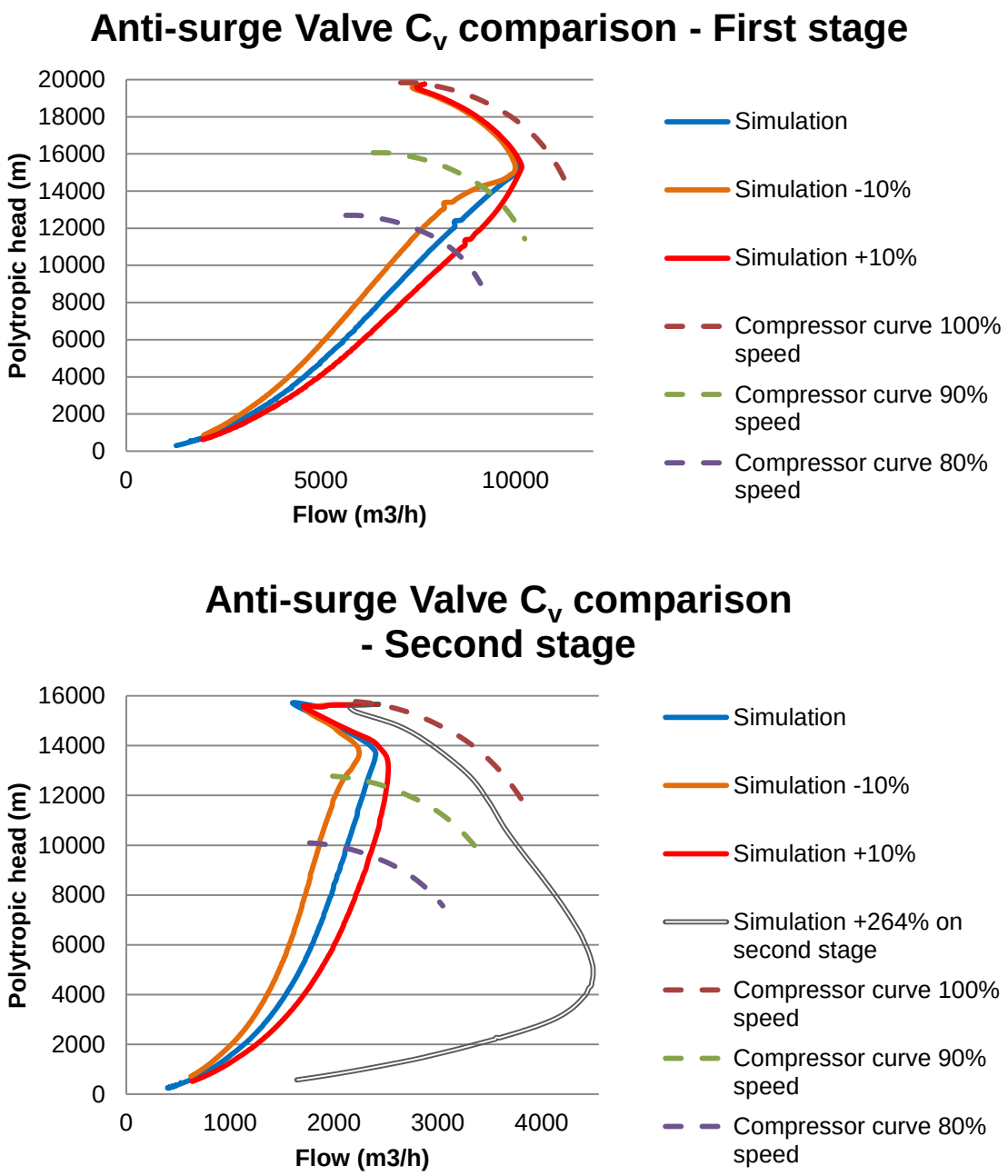

Figure 17 Compressor performance when anti-surge valve size is varied during shutdown from normal production at 10% surge margin.

As can be seen, larger valve size means that the flow through the compressor can be restored faster and thus the tendency to surge is reduced. With this being said, this effect was small and not enough to keep the second stage compressor from going into surge. This means that the preliminary C_v value does not appear to be large enough to avoid surge for the given surge margin and other parameters. In order to suggest another valve size that by itself would keep the second stage from going into surge, significantly larger C_v:s were simulated for the second stage and can also be seen in Figure 17. Simulations suggested that an increase of around 264% from the preliminary recommended value is the size that by itself would avoid surge. This value does however result in another problem – the flow becomes too large after the initial drop and would in reality reach the stonewall limit of the compressor. As seen in Figure 17, the simulation did not incorporate the effect of stonewall, thus the software extrapolates

compressor performance outside the supplied curve data. In terms of damage to the compressor, surge is a more severe problem than stonewall. A too large valve would however also result in a more complicated task for the anti-surge control, which limits the size that is practically possible to use.

The inertia of the compressor is another important factor for the risk of surge during shutdown as it affects the time taken for the compressor to lose speed. A higher inertia is expected to lead to a slower loss of speed and thereby a more stable behavior during shutdown, while the opposite is true for a lower inertia. As there is no data for the inertia of the new compressor, an evaluation of changes in inertia from the value of the existing compressor is shown in Figure 18. The rollout speed is also affected by the motor, gearbox and rotor friction factor but not to the same extent as the inertia. As a 100% reduction means that no inertia for the rotor would be modeled, the reduction was instead set to -50% in order to give meaningful results.

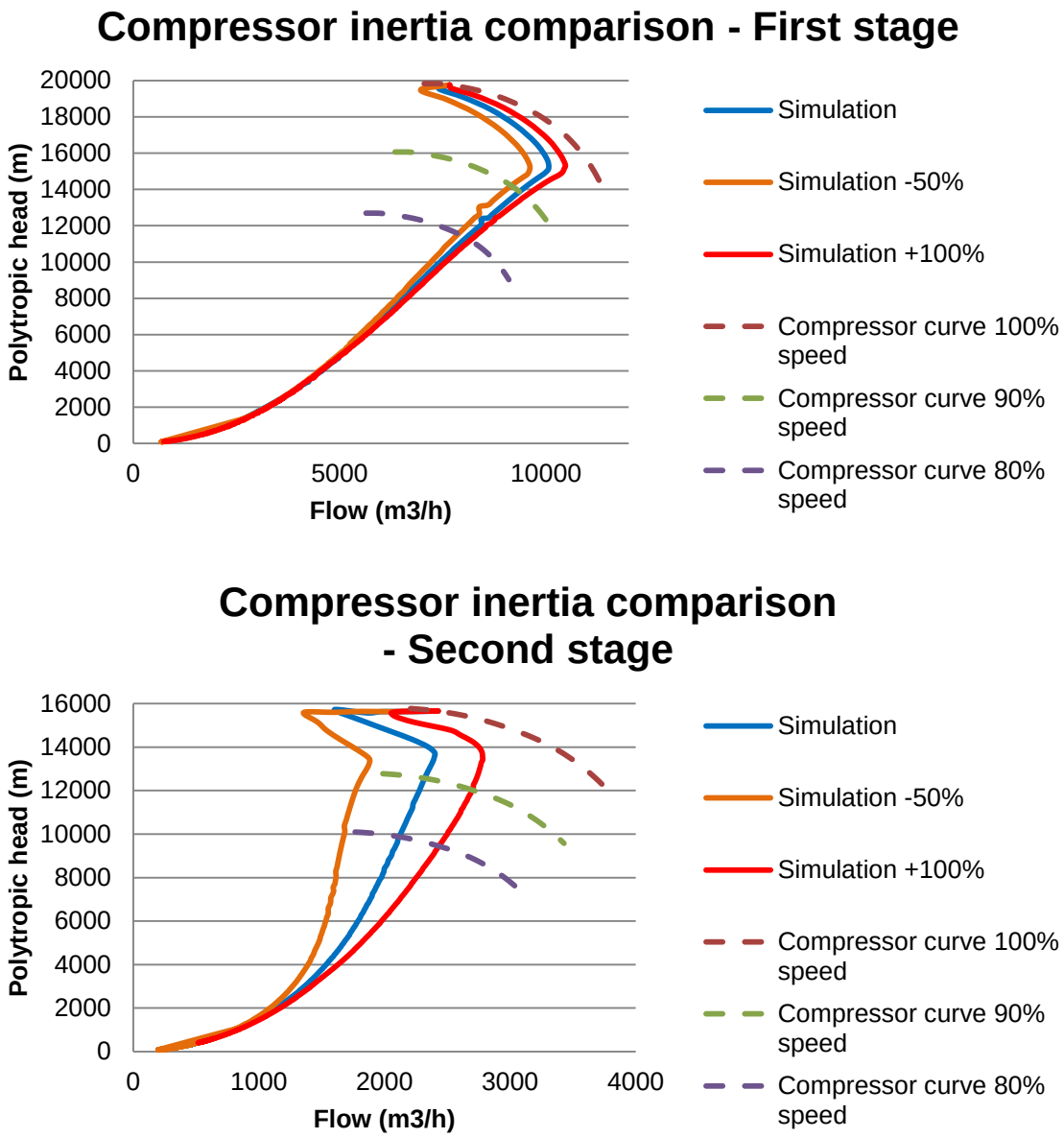

Figure 18 Compressor performance when the inertia of the compressor is varied during shutdown from normal production at 10% surge margin.

In Figure 18 the positive effect of an increased inertia can be seen as more time is available for the anti-surge valves to restore flow from the initial drop. The increased inertia will however also affect the start of the compressor. The extra weight will have to be accelerated and the start will take longer time and/or need higher power, which put extra requirements on the motor. This is investigated further in scenario B, where start-up is simulated for different inertias.

The volume on the discharge side is also expected to influence the anti-surge system, as the speed in which the fluid can circulate back to the compressor inlet is affected. Generally, one tries to minimize this volume by placing the anti-surge valves as close to the compressor discharge as possible in order to minimize the piping required. Figure 19 illustrates the result from simulations using the volume in the existing compressor system, as the volume for the reconstruction was not yet determined at the time of simulations. There have been suggestions to a change in the piping that would decrease the discharge volume of the second stage.

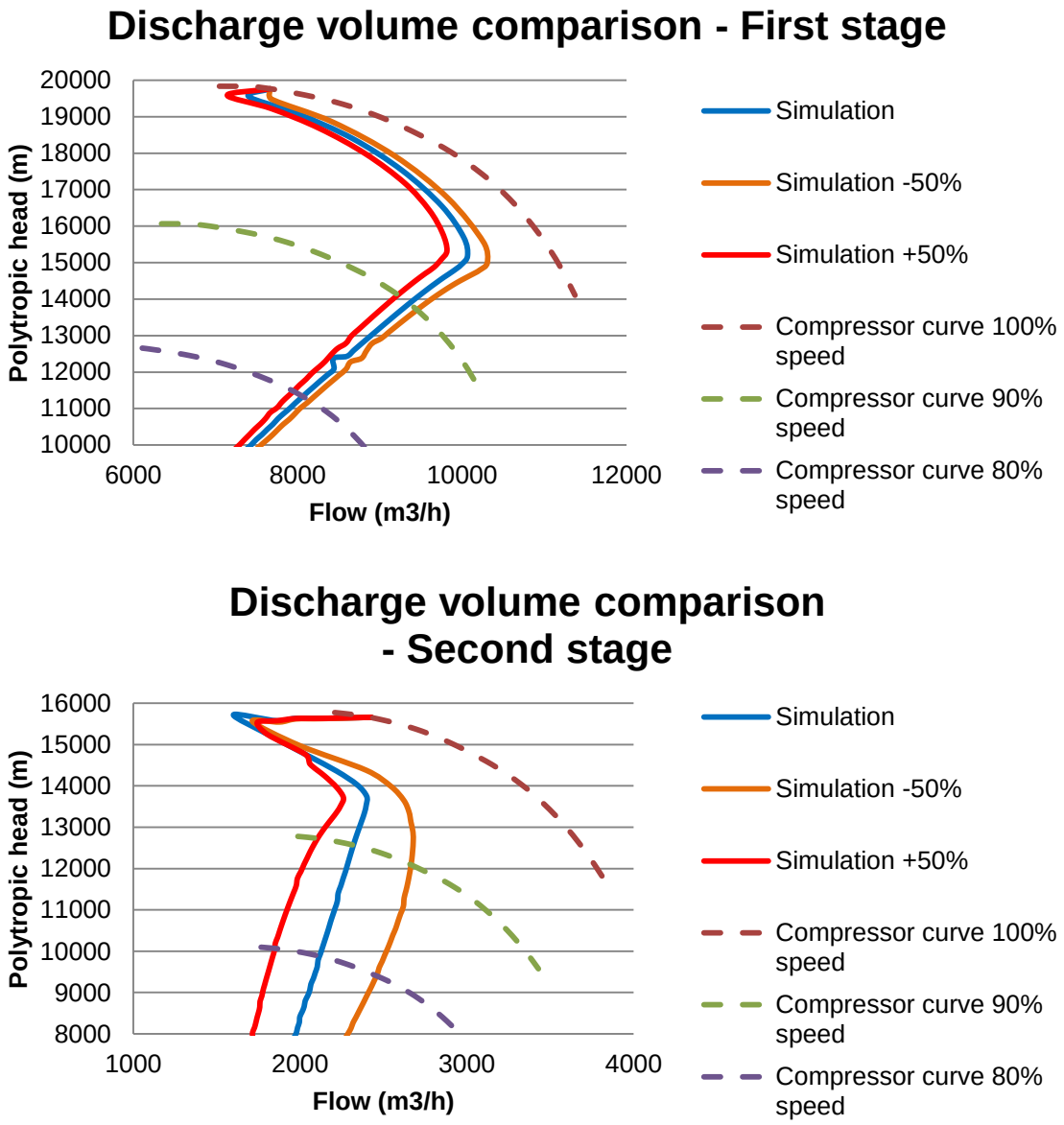

Figure 19 Compressor performance with varied discharge volume during shutdown from normal production.

As can be seen in Figure 19, the margin to surge increases with lower discharge volume as expected for the first stage. The first stage does not surge for any of the simulated volumes, but it can be seen that the margin to surge during the shutdown decreases as the volume increases. For the second stage however, both an increase and decrease in discharge volume seems to give a marginal reduction in the time spent in the surge area. HYSYS extrapolation and simulation performance in the surge area is known to be less reliable than inside the performance area defined by the compressor curves and this means that this result could be questioned.

The final evaluation of the anti-surge performance during shutdown is the anti-surge valve actuator opening speed. During shutdown of the safety system these valves are automatically set to fully open and the time needed for this is set entirely by the actuator stroke time. A faster opening means faster response by the anti-surge system and should therefore reduce the risk of going into surge. The result from evaluating the actuator opening speed ± 50% from the fastest speed suggested in the new *Modified* design is shown in figure 4. A comparison of the system with an ideal case of instantaneous anti-surge valve opening is also shown.

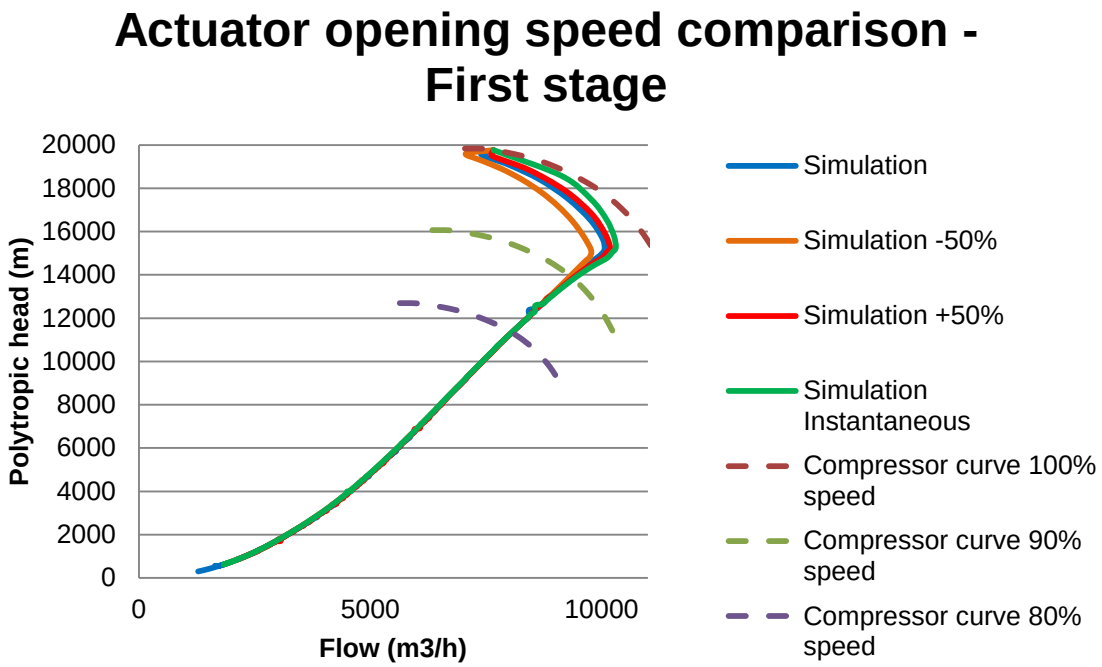

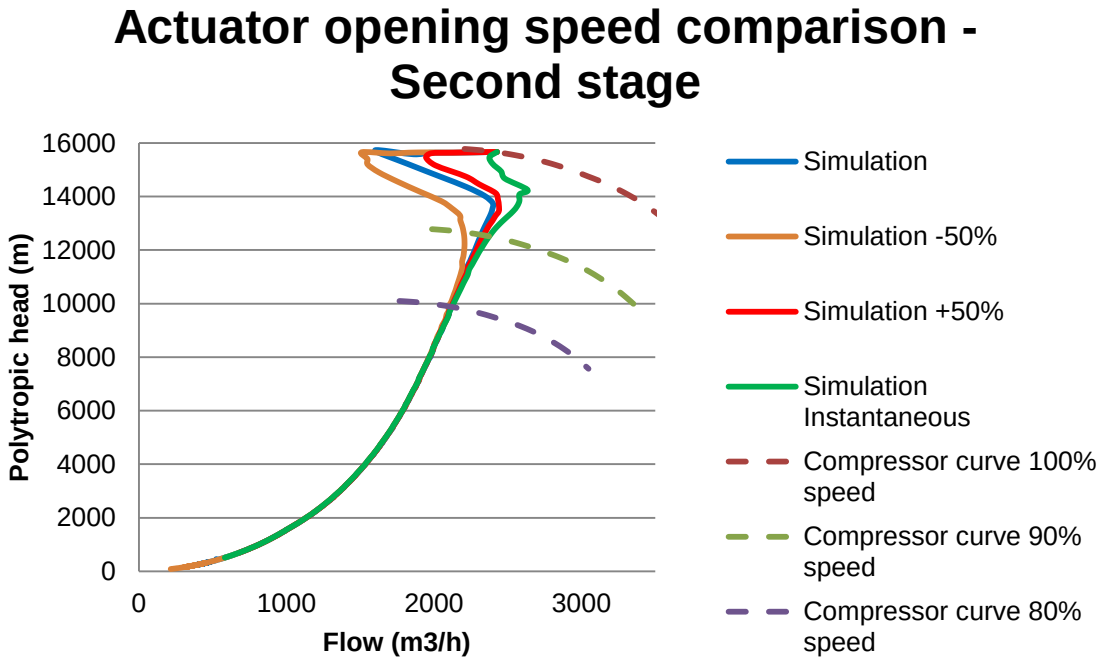

Figure 20 Comparison of compressor performance when varying anti-surge valve opening speed. Shutdown is performed from normal production at 10% surge margin.

Opening speed does impact the anti-surge performance significantly, but for the second compressor stage the ± 50% cannot prevent surge by itself. Instantaneous opening does however prevent surge, which was expected and means that it is possible to find an opening time that just barely avoids surge. As the base case simulation was set to the fastest speed suggested (full opening in 0,5 s), it is not as realistic to increase this speed with 50% and definitely not to have instantaneous opening.

In Figure 21 the shutdown event for the second stage at 10% surge margin is shown with a combination of the previous improvements in order to show that the suggested

improvements can result in a surge-free second stage during shutdown. This is done with the existing compressors inertia, as this parameter is based on the size of the compressor rotor and it was seen as the least realistic parameter to change in order to avoid surge. The combination is not necessarily optimal, but it is one possible solution to avoid surge on the second compressor stage. The C_v was increased with 30%, the opening speed was doubled and the discharge volume was decreased by 50% while keeping the inertia at the value from the existing compressor.

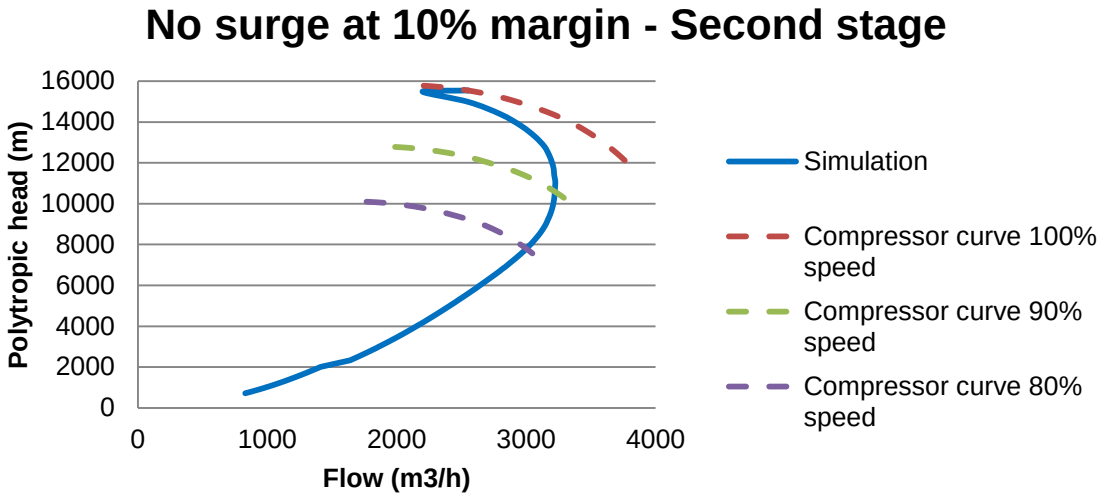

Figure 21 Second stage simulated with no surge by changing several parameters.

The data used to design the compressor system, in particular the second stage, has been proved to give surge during the shutdown simulations at normal surge margin of 10%. In Figure 21 it is shown that it is possible to get a more stable system by changing some of the given data. There are several possibilities as to why the original design data gave this unwanted behavior. As some of the data was not available and instead based on the assumption that it was similar to the old compressor, it was not completely accurate. Additionally it was seen in the validation chapter that the simulations could potentially overestimate the tendency to surge.

The general result from varying the parameters illustrated in Figure 16 to Figure 20 is that they all do have an observable impact on anti-surge performance and that the effects are more significant for the second stage compressor in all cases. When designing an anti-surge system it is of course important to optimize all these parameters for the given conditions and criteria's. Another possibility is obviously to increase the surge margin during operation.

5.2 Scenario B - Start-up

The following scenario simulates the start-up of the modified version compressor system from being shutdown up to full speed (10378 rpm) as described in chapter 3.3.2. Fluid and motor torque, start-up time and the pressure trend during startup are compared and evaluated.

In Figure 22 the fluid torque is shown as a function of speed during the start-up for simulation with the affinity laws (top) and with HYSYS linear extrapolation (bottom). The motor torque curve used is the same curve as for the old motor, and the inertia of

the compressor is the same as for the old compressor. The difference between the simulated fluid torque and the motor torque curve minus losses is the torque available to increase the speed.

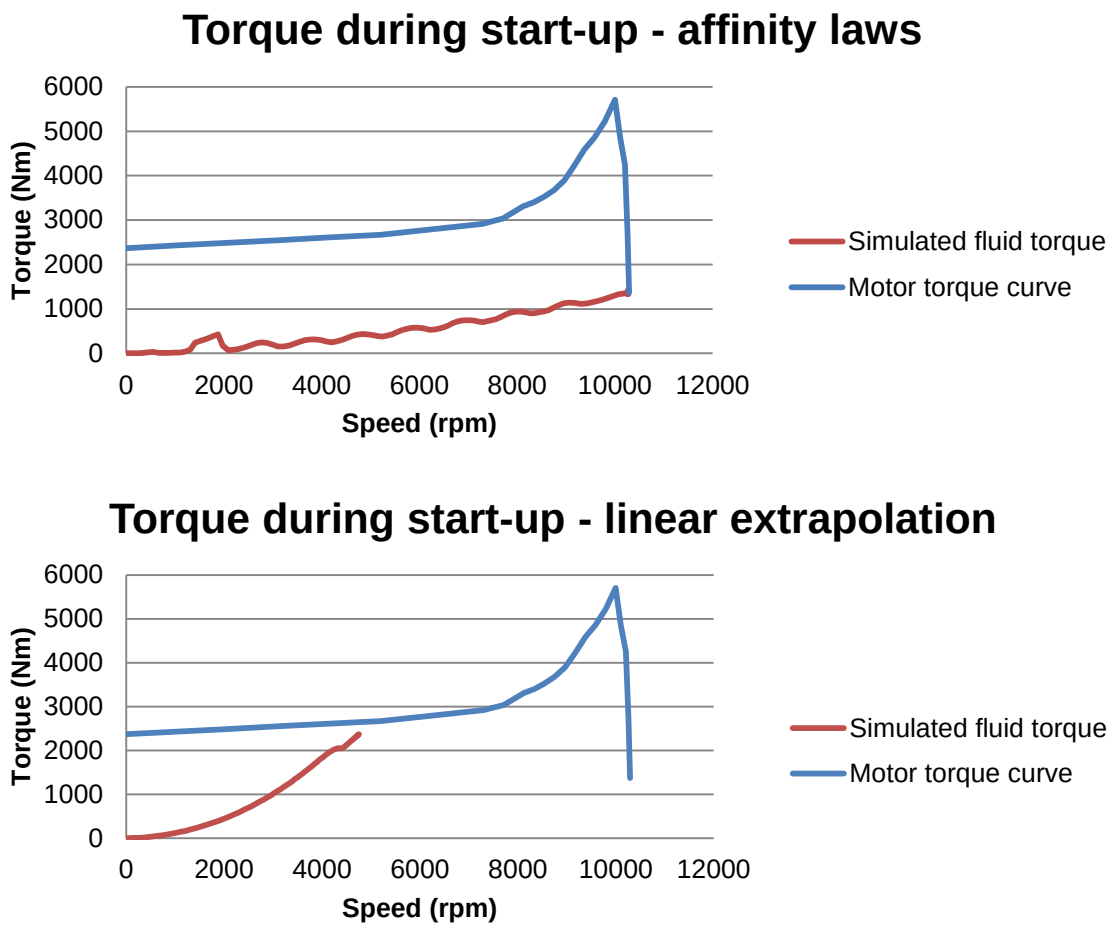

Figure 22 Fluid- and motor torque plotted during start-up using two different types of compressor curve extrapolations.

It can be seen that the fluid torque is very dependent on the method used to extrapolate the compressor curve. When the linear extrapolation (bottom chart) is used the compressor was not able to obtain full speed before the fluid torque curve reaches the motor torque curve. This is the result of a higher head for the same speed compared to the affinity law extrapolation, leading to a larger pressure rise and more energy given to the fluid rather than to accelerate the compressor. The molecular weight in the compressor is also an important factor, as if the molecular weight was lower the fluid torque for a given speed would also be lower and the compressor would possibly be able to start up.

When the affinity laws were used the fluid torque is oscillating as a result of the interpolation between the different compressor curves given to HYSYS. There is however a large margin between the fluid torque and the motor torque during the whole simulation and the effect of the oscillation should have a minimal effect on the compressor start-up time.

How long it takes to start the compressor is dependent both on how much torque that is available to increase the speed and on the inertia of the system. A high inertia means a

high resistance to change in motion and thereby a longer starting time. As seen in equation 6 the starting time is linearly dependent on the inertia if the torque of the compressor is constant. In Table 5 the starting time is shown for different compressor inertias and torque curves. Keep in mind that the inertia of the motor is the same in all simulations. It can be seen from the table that the startup time indeed is close to linearly dependent on the inertia.

Table 5 The time needed to reach full speed for different compressor inertias and motor torque curves.

Starting time	*Existing inertia -50%*	*Existing inertia*	*Existing inertia +100%*
Existing torque curve	7 s	11 s	19 s
Estimated torque curve	6 s	9 s	15 s

The manufacturer had proposed a start-up time of 9 seconds as a rough estimation, which seems to fit well with the assumption of similar inertia between the new and the old compressor. This is especially true for the estimated torque curve. It is however not possible to determine which motor curve or what inertia is most probable as they are dependent on each other and because the given startup time is an estimation. Having said this, the simulated start-up time lies very closely to the manufacturer suggested value.

In Figure 23 the pressure is shown as a function of time during the startup of the system over both compressor stages. The simulation is done using the existing motor torque curve, but using the estimated torque curve yields similar results.

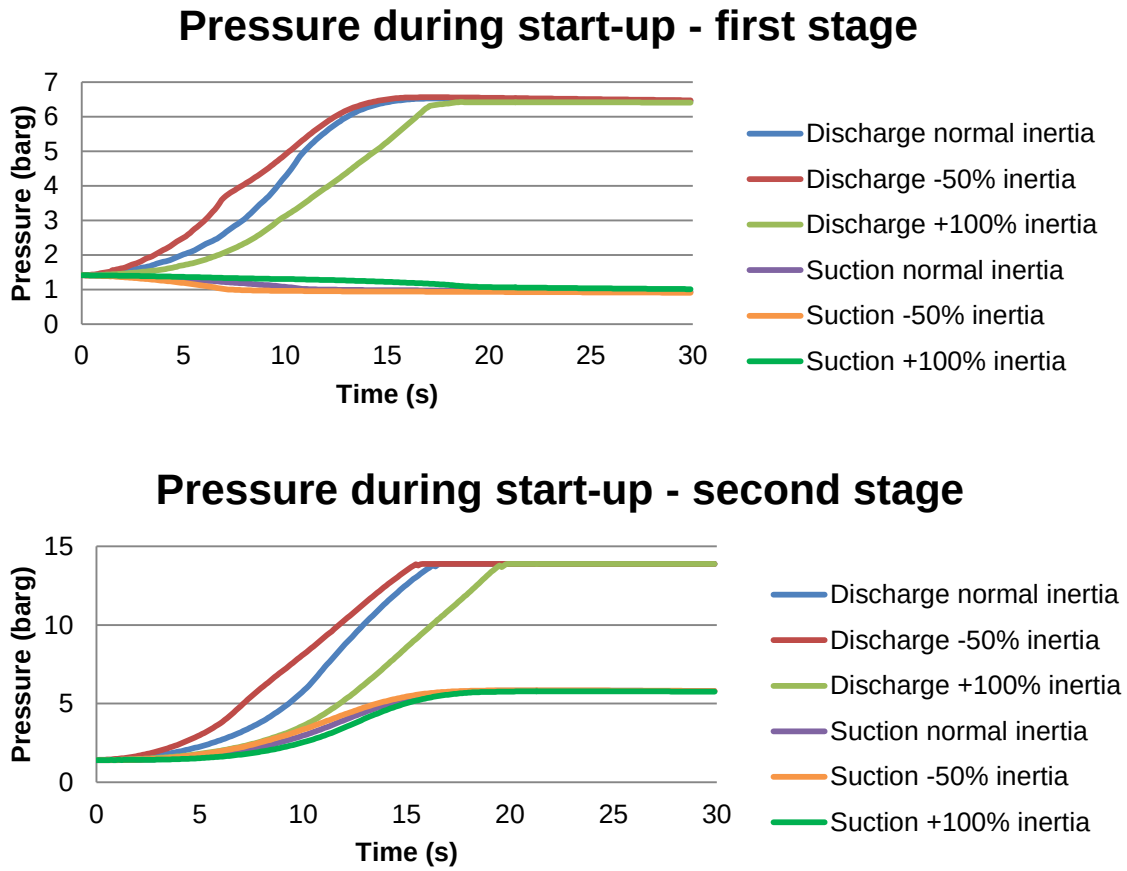

Figure 23 Pressure trend for outlet and discharge sides of both compressor stages during startup.

The pressure profile is similar for the different cases but the time to reach a steady state pressure is as expected longer for a higher inertia. It can be seen that the pressure continues to rise after the compressor has gained full-speed, the phenomena is most prominent for the lower inertias than for the higher. This indicates that the flow decreases and that the head increases (i.e. going left on the compressor curve) after full speed is reached. As the surge valve is fully opened during the startup the operating point reached by the compressor stages will be determined by the size of the surge valve. If the flow is much larger than what is set by the maximum flow in the compressor curve for any given speed this is likely because the compressor has reached its stonewall limit. The stonewall limitation is not simulated in the model and thus the flow can be higher in the simulation than what is realistically possible. If the flow was limited by stonewall it is expected that the polytropic efficiency decreases which leads larger temperature rise in the compressor stages. It is also expected that the pressure rise would be faster initially and closer to the steady state pressure when full speed is reached.

5.3 Scenario C - Step-change

This scenario focuses on the control of the compressor system, first in its entirety and then specifically the anti-surge valves. The scenario is described in greater detail in chapter 3.3.3 and is performed by simulating two different step-changes. The evaluation discusses both the process response and control parameters by observing flow and pressure trends.

The system did not reach any of the safety limits found in the safety system after any of the two step-changes. In Figure 24 the suction and discharge pressure of the first compressor as well as the suction pressure of the second stage are shown for both step-down and step-up of the inflow. The discharge pressure of the second stage is not shown as it is almost constant due to the gas pressure outlet boundary condition. The stability of these pressures is here used to determine the stability of the whole system, as changes in pressure travels quickly through the system.

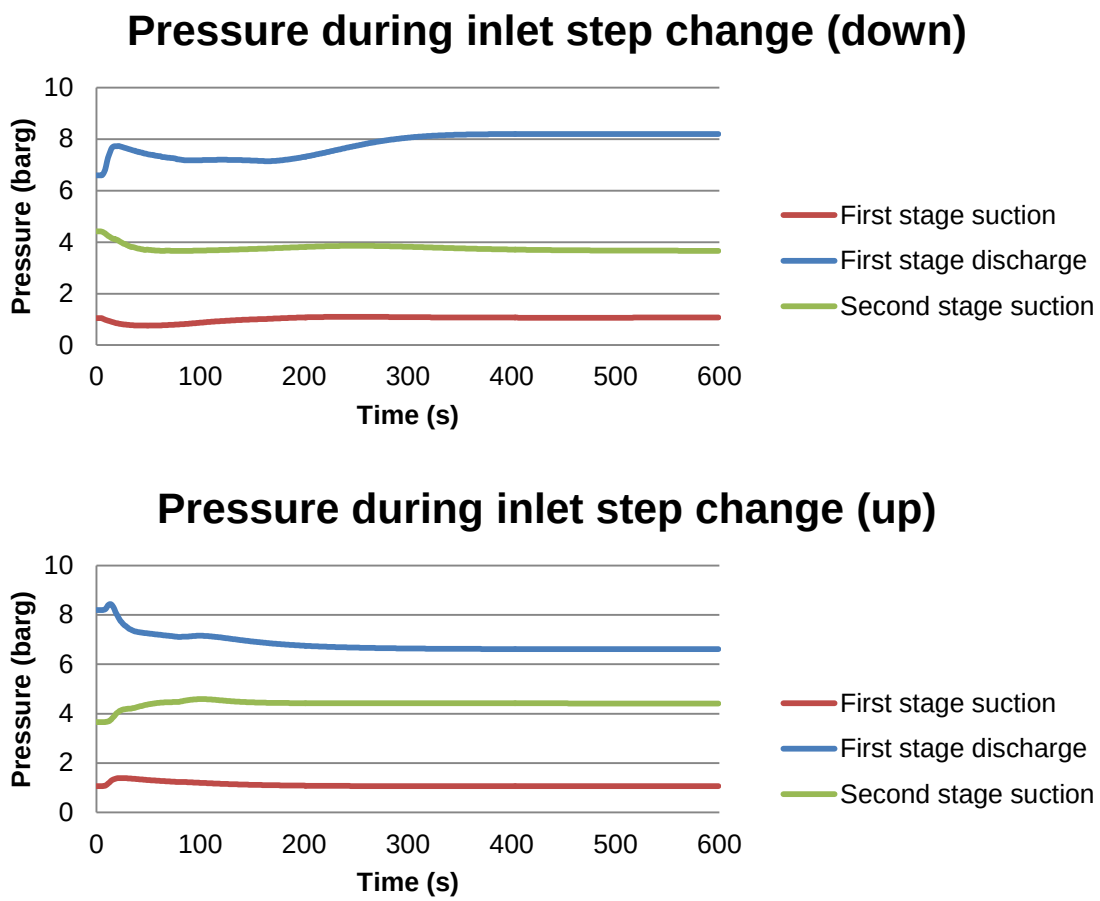

Figure 24 Change in pressure during step change scenario from simulation.

It can be seen that after about 300 seconds (5 minutes) after a step-change all the pressures has come close to steady state. The behavior does not indicate any instability, and even though there are some overshoot seen in the pressures these are never close to the safety limits. The difference in pressure between the discharge of the first stage and the suction of the second stage changes because of the change in molecular weight after the step-changes.

Figure 25 shows the flow through the compressor stages as well as the surge control line and the surge backup line for the downward step change simulation seen in Figure 24. This figure illustrates the ability of the system to avoid surge when the anti-surge control system active. The upward change is not included as there is no risk of surge when the flow is increased.

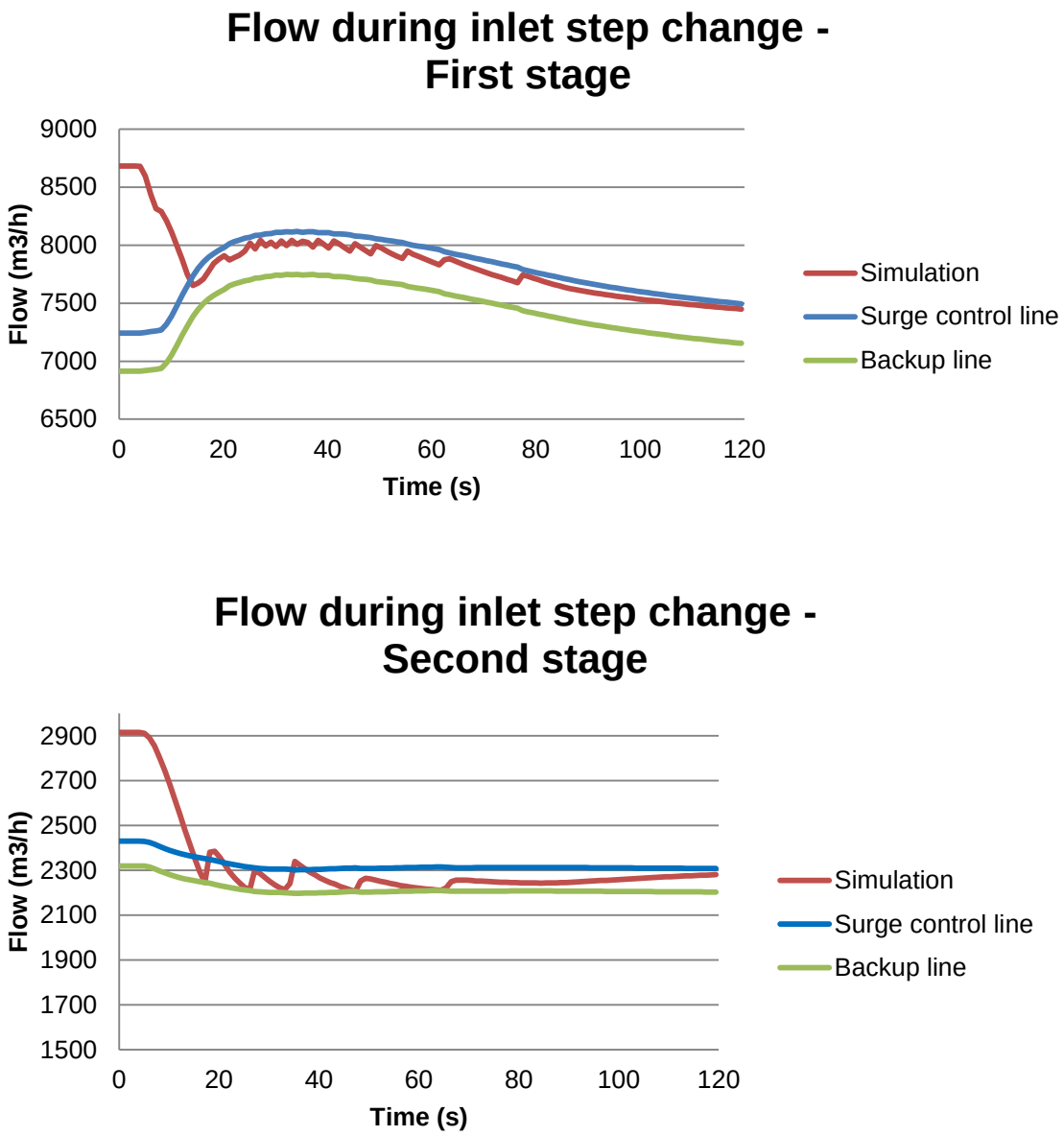

Figure 25 Flow simulation during downward step change of TSB inlet flow for both compressor stages.

The second stage oscillation is a result of this compressor stage repeatedly going into the backup line and triggering the more aggressive reaction from the anti-surge controller. It is evident that the system can be controlled with the used parameters. It is however also possible that the performance of the system could be improved by optimizing the control parameters. The advantage of this could be faster control and less overshoots.

In order to improve the control parameters beyond the rules of thumb values given by HYSYS one can perform various tuning procedures to ensure stable operation. These can be very rigorous and should be done accurately if one wishes to obtain optimized parameters. This type of rigorous optimization does however not lie within the scope of this report and thus no real "optimization" of the control system has been done. Instead, the following section illustrates how the system behaves differently as the control parameters in the anti-surge valves are varied. The plotted results are only shown for the

second stage anti-surge valve, as this valve showed the most critical behavior in the shutdown scenario evaluation in section 5.1.

The basis for comparison of the anti-surge control parameters will be the values suggested by HYSYS for PI-regulation of flow control (K_p=0,65 and T_I=0,25 min). The step change was done by changing the anti-surge valve controller set point (SP) from a 10% anti-surge line margin to a 30% margin. As only the proportional and integrating parts of the standard HYSYS PID-regulator is used in the model, only these parameters were varied. The overshoot, settling time and other characteristics can be seen in Figure 26 for simulations of the second anti-surge valve.

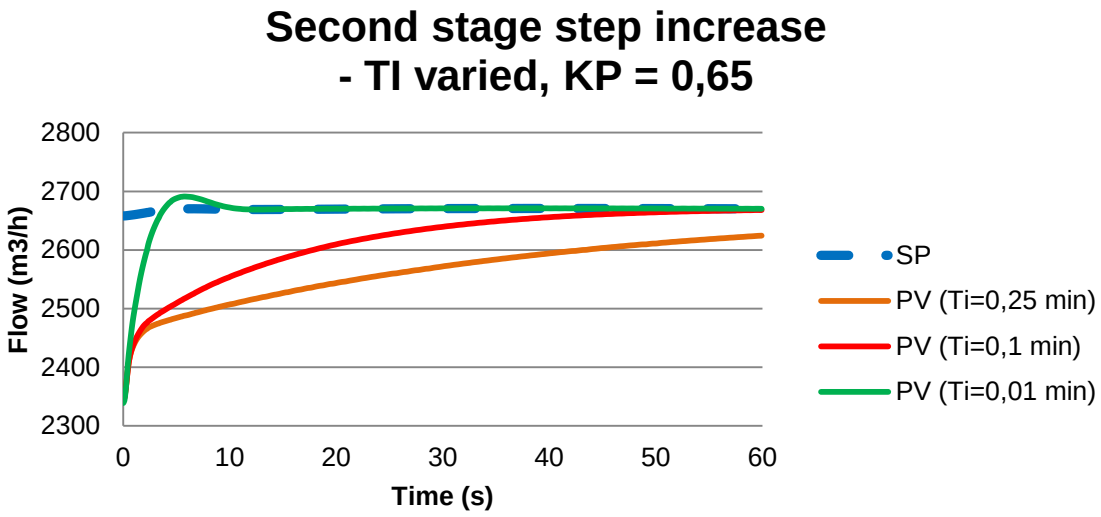

Figure 26 Step change response for the second stage anti-surge valve with constant K_P and varied T_I.

Both Figure 26 and Figure 27 show behavior that can be expected as T_I is reduced. As T_I is inversely proportional to the gain constant for the integrating term (K_I), a decrease in T_I should mean larger gain and longer settling time. The simulation does however show that the settling time is instead reduced when T_I is also reduced in Figure 26. This is explained by the fact that the base T_I is so large that overshoot is not present. If the base parameter had yielded a significant overshoot, then the reduction of T_I would have increased the overshoot amplitude and settling time. With the tested variables there are no significant signs of instability, even though a small overshoot can be seen for the smallest T_I.

It is not only the integrating factor but the combination of both K_P and T_I that defines the control system response for PI regulation. Because of this, K_P was varied while keeping T_I constant during the same step change procedure as before. The T_I value held constant was 0,01 min as this gave the best result from the comparison shown in Figure 26.

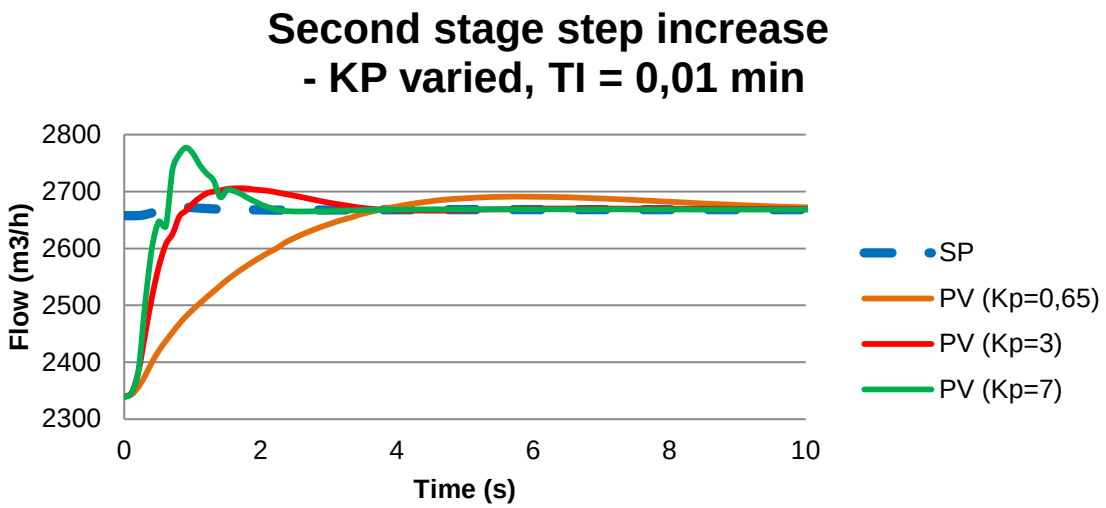

Figure 27 Step change response for the second stage anti-surge valve with constant K_P and varied T_I. Observe the shorter timescale compared to Figure 26.

Figure 27 illustrates that increasing the proportional gain constant K_P results in a faster response and shorter settling time. As mentioned in the theory chapter on PID regulation, this can introduce stability issues like the increased overshoot, which can also be seen in this figure. Among the tested values K_P =3 gives the best result, as it produces less overshoot but still a fast settling time.

A similar control parameter evaluation was done for the first stage anti-surge valve and the suggested values from this comparison can be seen in Table 6. This table also includes results from a Ziegler-Nichols parameter tuning and HYSYS suggested values for comparison.

Table 6 Comparison of PI controller constants suggested by various sources.

Parameter	HYSYS	Ziegler-Nichols First stage	Simulation First stage	Ziegler-Nichols Second stage	Simulation Second stage
K_P	0,65	0,64	6	1,4	3
T_I (min)	0,25	0,003	0,01	0,014	0,01

The values given in Table 6 do show significant variations, which is to be expected as both Ziegler-Nichols and HYSYS values are only meant to be rules of thumb. The values obtained from the simulation do improve the model control responsiveness. A comparison for the simulation step change response for the different models shown in Table 6 is presented as a graph in Figure 28.

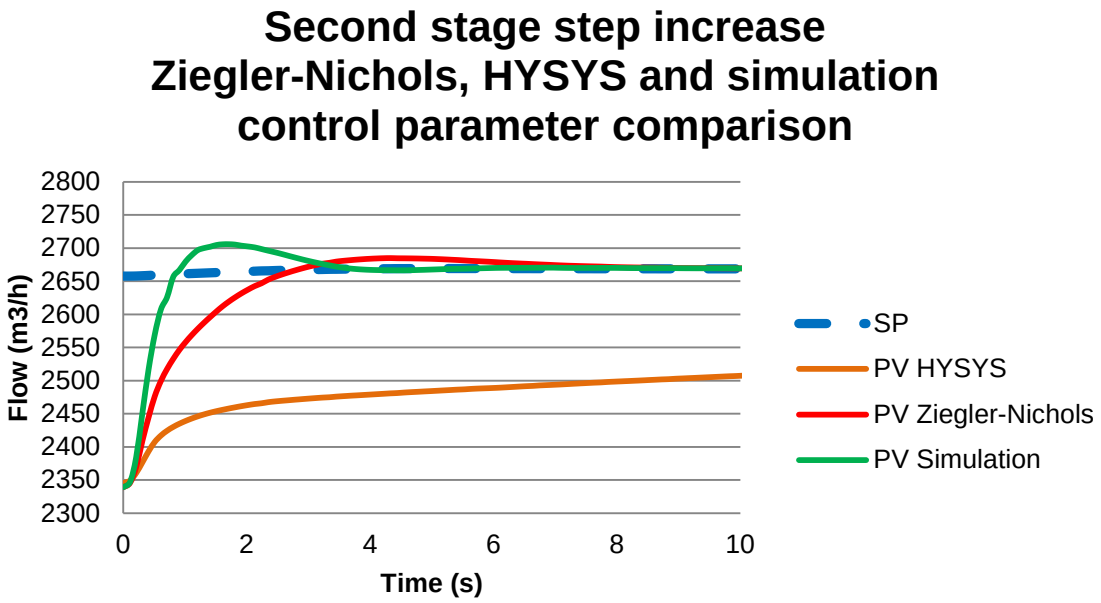

Figure 28 Comparison of the different rules of thumb control parameter suggestions during a step change from 10% to 25% surge margin.

This comparison gives an idea of the applicability of the rules of thumb in relation to tuning by "trial-and-error" in simulation for this specific system. This also illustrates one of the benefits of accurate dynamic models, as tuning can be done without affecting the operation of a real system. This is especially true when using a trial-and-error approach, or if it is hard to find stable control parameters of the system. The two control parameters examined in this thesis can however not be directly used in the proposed reconstruction when it is completed, as the type of anti-surge controller available in HYSYS is a simplification of what is being used in reality.

When the shutdown was investigated it was suggested that C_v needed to increase by about 264% (C_v =400) from the manufacturer suggested value (C_v =110) to solely avoid surge in the second compressor stage. In Figure 29 the step response of the system with the large valve is shown. The control parameters used are the Simulation parameters presented in Table 6.

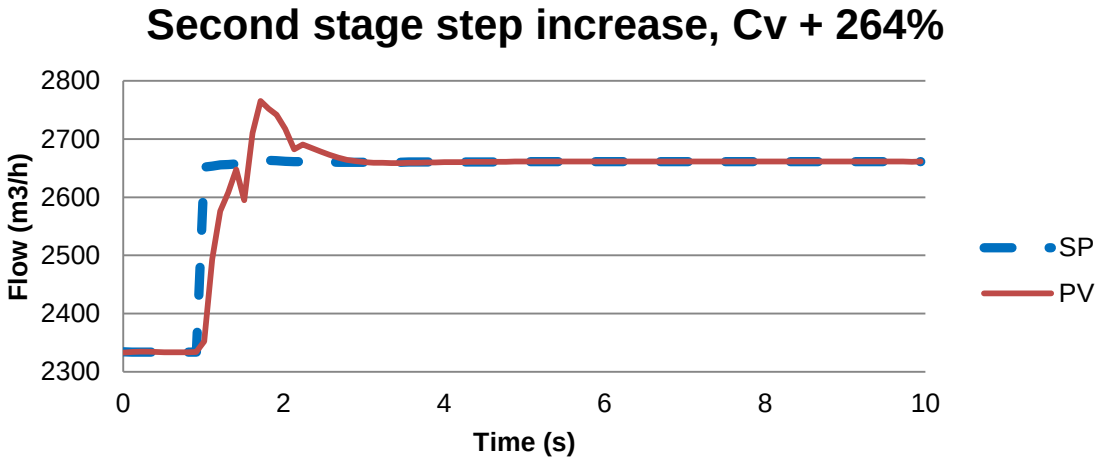

Figure 29 Step change response for the second stage anti-surge valve with an increased C_v value.

It can be seen that the controller is still able to eliminate the error and the response is very similar to the response with the highest K_P in Figure 27. This suggests that the valve is still controllable, and with the right control parameters can have similar performance as the smaller valve. This simulation has however not incorporated noises that can lead to worse performance. A larger valve is more sensitive to noises as small changes in the opening of the valve will give larger variations in the flow through it.

6 Conclusions

The validation did show that the model gave similar dynamic behavior as what is observed in reality for starting time, flow and pressures. The simulation of temperature could however be questioned and would need to be simulated with external heat transfer and accumulation in order to be used for drawing conclusions. The validation also resulted in faster dynamics than in reality, meaning that for example the tendency to surge can be overestimated.

The modified version simulation results showed that the modified system has problems with surge at the second stage during shutdown. When the anti-surge control system is active, surge is however prevented by the more aggressive backup line action. Even though no exact solution was proposed it is reasonable to suggest a higher C_V for the 2nd anti-surge valve. This can be combined with the other improvements shown in Scenario A, but additional investigation would be good in order to determine how critical the need is as the model may overestimate the surge tendency.

The start-up simulation did show how the start-up is dependent on inertia and on the extrapolation of compressor curves at different compressor speeds. It was shown that the new compressor could have problems to start-up if its actual compressor curves at lower speed are similar to the default extrapolation used by HYSYS. The real start-up time could not be determined as there were too many uncertainties, but if the affinity laws are somewhat realistic the simulated start-up time of around 10s seems probable. This is also in line with the given value for the start-up time from the manufacturer which gives additional validation to these results.

The step-change scenario did show that the compressor system is very stable and thereby easy to control. Even with a very rough estimation of the control parameters the system showed small to none signs of instability. It was also showed that the model could be used to increase the performance of the control system in a simple fashion. The anti-surge controller available in HYSYS was not modeled specifically after the real controller, which means the proposed control parameters do not have to be directly applicable to the real system.

All of the simulations also show benefits of using dynamic simulations in general when designing and optimizing this type of systems. When the model is created it is easy to make changes in the data and to test different scenarios without having to put much time or resources into it. Having said this, care must be taken to HYSYS default compressor curve extrapolation as this tends to overestimate the head increase at low speeds. Surge modeling is also handled poorly by the software and stonewall behavior can only be defined for one specific compressor curve, making it impossible to simulate stonewall for different compressor speeds or molecular weights.

7 References

- ANSYS, 2009. *Ansys 13 CFX modelling guide,* Southpointe: Ansys, inc.
- Aspen Technology, Inc., 2011. *Aspen HYSYS - Dynamic Modeling Guide,* Burlignton: Aspen Tech.
- Aspen Technology, Inc., 2011. *Aspen HYSYS - Unit Operations Guide,* Burlington: Aspen Tech.
- Bloch, H. P., 2006. *Compressors and Modern Process Applications.* Hoboken, New Jersey: John Wiley & Sons.
- Brown, R. N., 2005. *Compressors: selection and sizing (3rd edition).* Amsterdam: Elsevier.
- Brun, K. & Nored, M. G., 2008. *Appliaction Guideline for Centrifugal Compressor Surge Control Systems - Realease Version 4.3,* Dallas: s.n.
- Cheung, T.-F. & Luyben, W. L., 1979. Liquid-Level Control in Single Tanks and Cascades of Tanks with Proportional-Only and Proportional-Integral Feedback Controllers. *Ind. Eng. Chem. Fundam.,* pp. 15-21.
- Devold, H., 2010. *Oil and gas production handbook.* Oslo: ABB Oil and Gas.
- Fisher Controls International, 2005. *Control Valve Handbook.* 4th ed. USA: Fisher Controls International.
- Glad, T. & Ljung, L., 2009. *Reglerteknik - Grundläggande teori.* Lund: StudentlitteraturAB.
- Golden, S. W., 2002. Understanding Centrifugal Compressor Performance in a Connected Process System. *Petroleum Technology Quarterly.*
- KLM Technology Group, 2011. *Compressor selection and sizing (Engineering Design Guidline).*. [Online]
  Available at:
  http://kolmetz.com/pdf/EDG/ENGINEERING%20DESIGN%20GUIDELINES%20-%20Compressors%20REV02.pdf
  [Accessed 11 March 2013].
- Lapina, R. P., 1982. How to use the performance curves to evaluate behavior of centrifugal compressors. *Chemical Engineering,* p. 86.
- O'Hearn, T., 2013. *Calculating Motor Start Time,* s.l.: PDHonline.org.
- Peter C. Rasmussen, R. K., 2009. *Centrifugal Compressor Applications - Upstream and Midstream.* Houston, Texas, Turbomachinery Laboratory, pp. 169-186.
- Riviera, D. E., Morari, M. & Skogestad, S., 1986. Internal Model Control. 4. Pid Controller Design. *Ind. Eng. Chem. Process Des. Dev.,* pp. 252-265.
- Sinnott, R. & Toweler, G., 2009. *Chemical Engineering Design.* 5th ed. Burlington: Elsevier Ltd..
- Sulzer Chemtech Ltd, 2009. *Gas/Liquid Separation Technology,* Winterthur, Switzerland: Sulzer Chemtech Ltd.
- Vinod Patel, J. F. S. D. P. R. a. J. W., 2007. *Application of dynamic simulation in the design, operation and troubleshooting of compressor systems.* Houston, Texas, KBR, Inc.
- Welty, J. R., Wicks, C. E., Wilson, R. E. & Rorrer, G. L., 2008. *Fundamentals of Momentum, Heat, and Mass Transfer.* USA: John Wiley & Sons, Inc..

Appendix A – Complete flow sheet of the simulated process

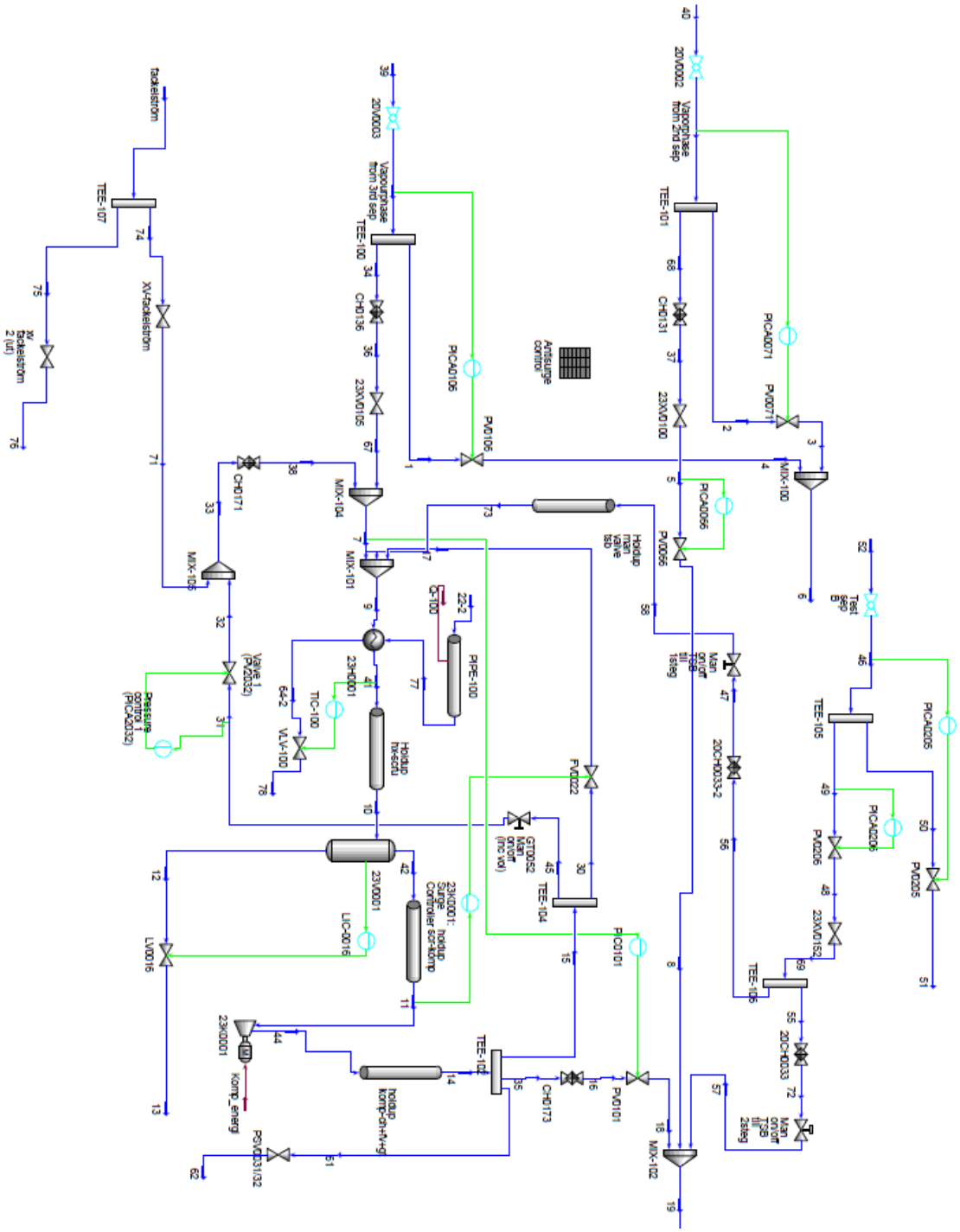

Figure A1 Flow sheet of the simulated model, part 1. The first compressor stage and all system inlets are shown. The outlet stream (19) is the inlet stream the second part of the flow sheet.

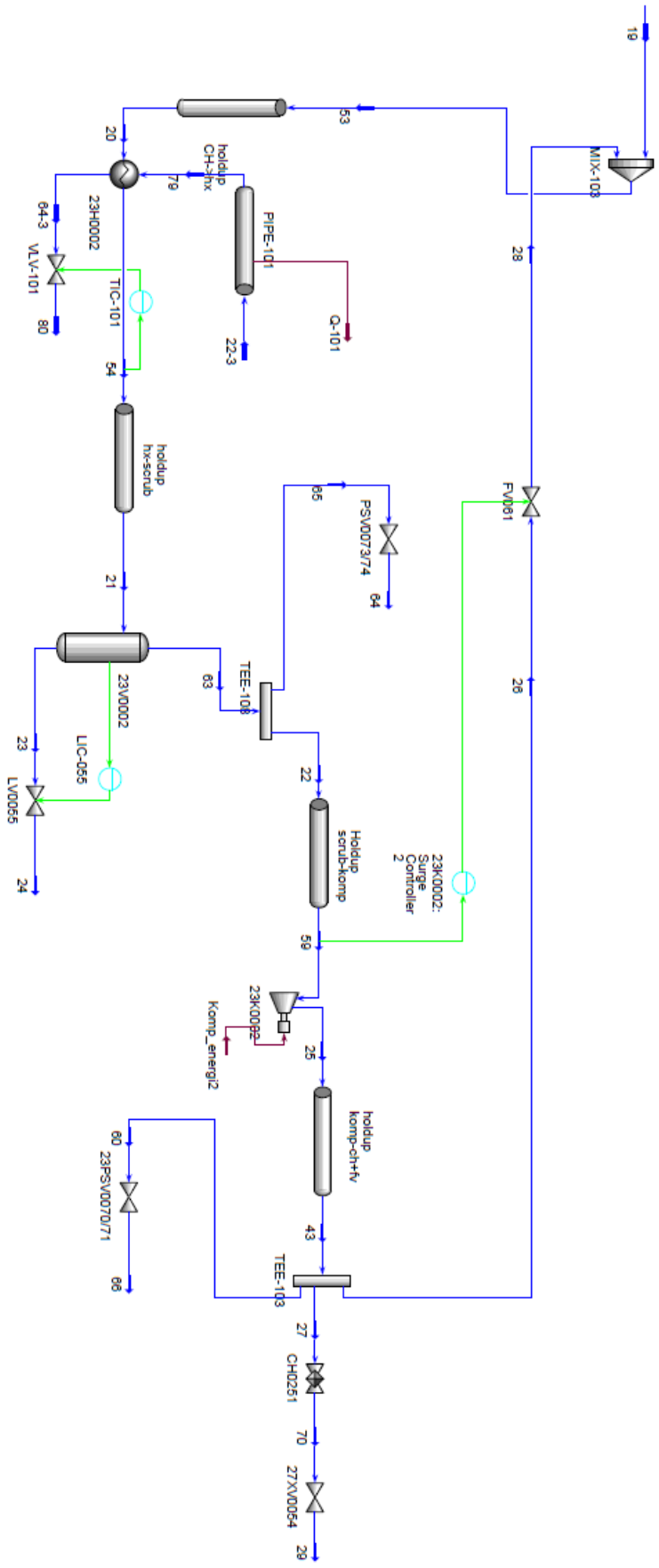

Figure A2 Flow sheet of the simulated model, part 2. The second compressor stage is shown. The inlet stream (19) is the outlet stream the first part of the flow sheet.

Appendix B – The control system

This appendix includes information on the purpose of the different controllers in the simulated control system. This is important information in order to get a more comprehensive understanding on how the system works. It also contains information on which control parameters that were used for the different controllers.

The control system consists of a total of 13 different controllers which all can be seen in the flow sheet in appendix A. These include two anti-surge controllers, one liquid-level controller for each scrubber and one temperature controller for each heat exchanger, three flare controllers (one for each separator), pressure controllers for the flow into the system from the 2nd stage separator and TSB, one controller regulating the valve (PV0101) between the compressor stages and one controller for the flare recycle flow. Most of these controllers are very straight forward, with the possible exception of the anti-surge control, the flare recycle and the controller of PV0101.

As the anti-surge control has been covered quite extensively in the report it will not be focused on here, even though it is the most complex controller of the control system. The anti-surge controllers regulate recycle valves from the discharge to the suction of the compressor stages (actually to the pre-cooler). This is done in order to be able to avoid a too low flow into the compressor, as that can lead to surge and damage to the compressor. It is critical that the anti-surge control and valves are fast in order to be able to raise the flow fast enough in an event of decreased inlet flow.

The liquid level in the scrubber is controlled by regulating the liquid outlet of it. The liquid level is not important for the simulations done in this report, as long as the level is kept below the vapor outlet nozzle. The temperature control measures the temperature at the process media outlet and regulates the cooling media flow through the heat exchanger. The purpose of the flare controllers is to avoid a too high pressure in the separators, so when the pressure increases above the set point the route to flare is opened. The pressure controllers from the 2nd stage separator and TSB control the pressure in the separators.

The controller of PV0101 is actually regulating the pressure out from the 3rd stage separator. If the pressure is too low out of the separator the valve between the stages will close and the pressure will increase in the whole system up to the valve. The reason this is not controlled in the same way as for the other separators is because the risk of getting a too low pressure in the suction of the first stage, with possible leakage of air into the system as a result.

The flare recycle controller is the only controller in the system that actually does not exist in the same fashion in reality as in the simulation. This is a result of how the system boundaries were drawn. In reality the pressure of the flare recovery stream is raised with the flare recycle stream from the 1st stage discharge in an ejector. The ejector comes with pressure controllers to determine the pressure and flow through it, but it was however outside the simulated system boundaries. The new flow controller was added in order artificially keep the flare recycle stream inside the system

boundaries instead of having a separate inlet and outlet for it. The set point was determined by taking a typical value of the flow of the recycle stream.

The control parameters used for all these controllers were based on the recommended intervals given in the HYSYS manual, see table B1.

Table B1 Recommended control parameters from the HYSYS manual

	K_P	T_I
Liquid level control	2-10	1-5
Gas pressure control	2-10	2-10
Temperature control	2-10	2-10
Flow control	0,4-0,65	0,05-0,25

The middle points of the intervals were used in all controllers with the exception of the three flow controllers. The anti-surge controllers were instead given the most aggressive values as the anti-surge system is known to have high requirements when it comes to speed. The flare recycle controller was not stable with the values suggested, so K_P was instead set to 0,2 and T_I to 0,4 as this gave stable behavior of the controller.

Appendix C – Anti-surge control: Reduced parameters

In order to simplify the anti-surge control in the HYSYS simulations performed in this report, the parameters of head and flow are reduced according to equation 17 and 18 in order to make the head versus flow coordinate system invariant to changes in inlet conditions.

$$h_r \equiv \frac{\frac{P_{discharge}}{P_{suction}} - 1}{\frac{(k-1)}{k\eta_p}} \qquad \text{C1}$$

$$q_s^2 \equiv \frac{Q_s^2(MW)}{Z_s R_u T_s} \qquad \text{C2}$$

h_r = reduced head
q_s = reduced flow
(MW) = molecular weight
Z_s = suction compressibility factor
R_u = universal gas constant
T_s = suction temperature (absolute)
η_p= polytropic efficiency
k = ratio of specific heats $\left({C_p}/{C_v}\right)$

It should be noted for real applications, real-time information on molecular weight and compositions are generally not available and therefor the reduced flow is calculated using the pressure differential over a compressor. The calculation of reduced head is also simplified by assuming constant ratio of specific heats (k). (Bloch, 2006)